

**An In-vitro Analysis of the Effects
Of Firocoxib on the Equine
Gastric Microbiome**

by

Gisselle Patricia Garcia Perez

A thesis submitted to the Faculty of the University of Delaware in partial fulfillment of the requirements for the degree of Honors Bachelor of Science in Pre-Veterinary Medicine and Animal Biosciences with Distinction

Spring 2019

© 2019 Gisselle Patricia Garcia Perez
All Rights Reserved

**An In-vitro Analysis of the Effects
Of Firocoxib on the Equine
Gastric Microbiome**

by

Gisselle Patricia Garcia Perez

Approved: _____
Amy Biddle, PhD
Professor in charge of thesis on behalf of the Advisory Committee

Approved: _____
Tanya Gressley, PhD
Committee member from the Department of Animal and Food Science

Approved: _____
Kalmia Kniel, PhD
Committee member from the Board of Senior Thesis Readers

Approved: _____
Earl Lee II, Ph.D.
Deputy Faculty Director, University Honors Program

ACKNOWLEDGMENTS

Dr. Amy Biddle

Dr. Annie Renzetti

Albert Armstrong “Farmer Larry”

The WOMBATS

Biddle Lab

Dr. Gressley

Dr. Kniel

Helen of Troy

Kung Lab

ANFS Department

CANR SI

Undergrad Research Office

UD Honors Program

“Sandy”

TABLE OF CONTENTS

LIST OF TABLES	vii
LIST OF FIGURES	viii
ABSTRACT	xi
1 Introduction	1
1.1 Horses and Society	1
1.2 The Equine Gut.....	2
1.3 Equine Gastric Microbiome	3
1.4 NSAIDs	4
1.5 What is COX Inhibition?.....	5
1.5.1 Firocoxib/Equioxx.....	6
2 Methods	7
2.1 Experimental Setup	7
2.1.1 Time-course Preparation	7
2.1.2 Dosage Calculation.....	9
2.1.3 Sample Collection	12
2.2 Experimental Procedure	13
2.2.1 Sampling Procedure.....	14
2.2.2 Cell Count Procedure	15
2.2.3 HPLC.....	15
2.2.4 DNA Extraction.....	16
2.3 Data Analysis.....	17
2.3.1.1 Gas Production and pH.....	17
2.3.1.2 HPLC Analysis	17
2.3.1.3 Sequencing Analysis	18
2.3.1.4 Statistical Testing	19
2.3.1.5 DESeq.....	19
2.3.1.6 Jamovi ANOVA	20
2.3.1.7 Combining HPLC and Sequence Data for Analysis.....	20

3	Results	21
3.1	Experimental Observations	21
3.1.1	Gas and pH Data.....	21
3.1.2	Cell Count.....	22
3.2	HPLC.....	23
3.3	16S-rRNA Sequence Data and QIIME.....	29
3.3.1	JAMOVl.....	33
3.3.2	DESeq.....	35
3.4	Sequence Data and HPLC Correlation	37
3.4.1	Positive Correlation.....	37
3.4.2	Negative Correlation	40
3.4.3	Drug Affected Taxa Correlation Data	43
4	Discussion.....	47
4.1	Experimental Goals	47
4.2	Taxa Analysis	47
4.3	Interpreting Results by Metabolites.....	48
4.3.1	Glucose	49
4.3.2	Lactate	53
4.3.3	Formate.....	56
4.3.4	Acetate.....	60
4.3.5	Propionate.....	62
4.3.6	Butyrate	65
4.3.7	Sulfur-Reducing Bacteria	68
5	Conclusion.....	70
5.1	Conclusions	70
5.2	Future Directions	71
	REFERENCES	73
A	MEDIA AND STANDARD PREPARATION	79
B	HPLC PROTOCOL.....	81
C	DNA EXTRATION PROTOCOL	82
D	QIIME SAMPLE SUMMARY	83

LIST OF TABLES

Table 1: Results of the paired t-test illustrating the values that were compared to a p-value of 0.05. Statistically significant differences were highlighted. Missing time-points did not have any detected metabolite concentrations and were excluded from the table.	27
Table 2: The 43 significant taxa groups are summarized. Taxa with an * were the taxa excluded from Figure 14 due to their relative abundances being less than .01% throughout the entire time-course.	30
Table 3: The 43 important taxa and the p-value generated by the JMV ANOVA. p-values less than 0.05 were considered significant. Taxa are colored by phyla according to Figure 2. Taxa with a * were excluded from abundance figures because they had less than .01% abundance throughout the time-course.....	34
Table 4: 43 important taxa as well as the p-value generated by the JMV ANOVA. p-values less than 0.05 were considered significant. Taxa are colored by phyla according to Figure 2. Taxa with a * were excluded from abundance figures because they had less than .01% abundance throughout the time-course.....	35
Table 5: Taxa groups whose absolute abundances were significantly affected by dose.....	36

LIST OF FIGURES

Figure 1: Experimental Set Up	9
Figure 2: Gas Production over the time-course. Gas produced has a distinct “rotten egg” smell. Serum vials with the same designation were combined.....	21
Figure 3: Graphical representation of the pH measurements taken over the time-course. Serum vials with the same designation were combined in order to showcase the average trends.	22
Figure 4: Mock up of hemocytometer and numbers of cells counted per square. Total number of cells counted was 417. Average number of cells per square is the total divided by the number of squares, which was 16.	23
Figure 5: Glucose Production. Dose data was averaged after statistical analysis showing no significant difference between treatments. Average pH data was superimposed on the right axis.	24
Figure 6: Lactate Production. Dose data was averaged after statistical analysis showing no significant difference between treatments. Average gas volume data was superimposed on the right axis.	24
Figure 7: Formate Production. Dose data was averaged after statistical analysis showing no significant difference between treatments. Lactate production was superimposed on the right axis.	25
Figure 8: Acetate Production. Dose data was averaged after statistical analysis showing no significant difference between treatments. Lactate production was superimposed on the right axis.	25
Figure 9: Propionate Production. Dose data was averaged after statistical analysis showing no significant difference between treatments. Lactate production was superimposed on the right axis.	26
Figure 10: Butyrate Production. Dose data was averaged after statistical analysis showing no significant difference between treatments. Lactate production was superimposed on the right axis.	26
Figure 11: Average metabolites trends over the time-course.	27

Figure 12: Stacked bar graph illustrating 33 of the 43 important taxa and how their abundances change over the time-course and by treatment.	31
Figure 13: Taxa Abundance by Phyla in which <i>Other</i> is pale yellow, <i>Bacteriodes</i> is green, <i>Firmicutes</i> is bright blue, <i>Fusobacterium</i> is gray, and <i>Proteobacteria</i> is pink.....	32
Figure 14: Metabolic pathways of metabolites tracked via HPLC and drug affected taxa.	33
Figure 15: Taxa positively correlated with glucose over the time-course.....	37
Figure 16: Taxa positively correlated with lactate over the time-course.	38
Figure 17: Taxa positively correlated with formate over the time-course.	38
Figure 18: Taxa positively correlated with acetate over the time-course.....	39
Figure 19: Taxa positively correlated with propionate over the time-course.....	39
Figure 20: Taxa positively correlated with butyrate over the time-course.....	40
Figure 21: Taxa negatively correlated with glucose over the time-course.....	41
Figure 22: Taxa negatively correlated with lactate over the time-course.	41
Figure 23: Taxa negatively correlated with formate over the time-course.	41
Figure 24: Taxa negatively correlated with acetate over the time-course.....	42
Figure 25: Taxa negatively correlated with propionate over the time-course.....	42
Figure 26: Taxa negatively correlated with butyrate over the time-course.....	43
Figure 27: Drug Affected Taxa for Glucose.....	44
Figure 28: Drug Affected Taxa for Lactate.....	44
Figure 29: Drug Affected Taxa for Formate.	45
Figure 30: Drug Affected Taxa for Acetate.	45
Figure 31: Drug Affected Taxa for Propionate	46
Figure 32: Drug Affected Taxa for Butyrate.....	46

ABSTRACT

There has been an increase in the use of NSAIDs in human and veterinary medicine. Horses, which are hindgut fermenters and obligate herbivores, rely on a symbiotic relationship with gut bacteria in order to digest plant matter. Changing attitudes towards the horse have led to a rise in the use of NSAIDs to relieve everyday aches and pains ensuring that all horses, from backyard pets to elite athletes. There have been deleterious side effects noted with the long term use of NSAID's, notably the formation of gastric ulcers. Recently firocoxib has risen in popularity because it has fewer side effects than other, traditional NSAIDs. This study aimed to characterize the effects of firocoxib on the equine gastric microbiome. Gastric fluid was collected from a healthy horse and inoculated into anaerobic media and treated with three concentrations of the drug. Samples were taken over a 48 hour time-course. pH and gas production was also measured. These samples were analyzed with HPLC to track the concentrations of microbial metabolites produced throughout the time-course. 16S-rRNA sequencing was used to identify changes in bacterial populations. Statistical analysis to determine the significance of the variations seen in the data included correlations between the taxa and metabolites to characterize the effects that the drug had on the bacterial populations in the gut. The results from this pilot study indicate that firocoxib has a detrimental effect on the microbiome. The addition of firocoxib to the gastric environment resulted in a decrease in the production of metabolites, changes in the growth of 43 taxa groups with a dose effect seen in 20 groups.

Chapter 1

Introduction

1.1 Horses and Society

The horse and the role that it plays in human society has undergone many iterations in the six thousand years since their domestication.^{1,2} Humans first came into contact with horses about 50,000 years ago when they were hunted as a food source. Since that time they evolved into a valuable piece of machinery in agriculture and as a means of transportation up until the early to mid 19th century.² After the introduction of automobile technology and their rise in popularity, the horse was phased out of its role in agriculture and as the most common means of transportation and started to fulfill a new role in society as a pet that can be used for recreation.³ The majority of horses in the United States, 47.2% are used for “pleasure” while only 1.6% are used for racing.⁴ Interestingly enough, the racing industry is responsible for 10.6 billion dollar impact to the American economy with recreation or “pleasure” contributing about 11.8 billion dollars.⁵ Horses in the modern day occupy two very interesting niches in society, one being that of a pet and the other being a highly valued athlete. Regardless of whether the horse is used for recreation, racing, or a multitude of other activities including, showing, farming, or breeding, the community responsible for these animals is invested in their health and well being and a major aspect of equine health is their gastrointestinal tract.

1.2 The Equine Gut

The digestive tract of the horse is unique from most other mammals because they are non-ruminant herbivores. They are also oftentimes described as hindgut fermenters or monogastric herbivores.⁶ Generally monogastric animals have short digestive tracts and are able to breakdown, absorb, and convert nutrients into energy very quickly. As such their diets generally consist of feeds that are high in non-structural carbohydrates or sugars that are easily broken down and converted into glucose as well as other nutrients that are used to build and repair their tissues.

³Conversely ruminant animals maintain a symbiotic relationship with hundreds of thousands of bacteria, fungi, and protozoa that ferment structural carbohydrates and turn them into a form that the animal can easily utilize. Because of this fermentative process that the feed undergoes before it is absorbed ruminant animals have large rumens and long digestive tracts with a much slower rate of passage of digesta than monogastric animals. Horses are unique because they combine both types of digestive organizational systems into a hybrid system.

As previously mentioned horses are non-ruminant monogastrics or hindgut fermenters. Ruminant animals ferment the forages that they eat in a large, multi-chambered stomach known as the rumen. After the feed has been sufficiently fermented it moves into the true stomach which is the site of enzymatic digestion. From there it passes into the small intestine where any remaining nutrients are absorbed and then the digesta continues through the small and large intestines until it is expelled from the body. Unlike ruminants the forage that a horse eats first passes through the true stomach, which remains the site of enzymatic digestion. However mammals are unable to produce enzymes that can breakdown structural carbohydrates into readily accessible sugars, but bacteria are able to break these bonds and access the

energy stored in them. In horses this forage passes from the stomach into the small intestine and then into the cecum. Rather than having a multi-chambered stomach like ruminants horses have a large, blind ended pouch known as the cecum that acts as the site of this microbial fermentation. So while the bacteria are breaking down the beta glycosidic bonds that hold these structural carbohydrates together they are in turn producing these short chain fatty acids that the horse can use for energy. Horses can receive between 30% - 50% of their total energy requirements from this microbial fermentation.³ Once the forage has been sufficiently fermented it exits the cecum and continues through the rest of the large intestine until it is expelled from the body.

1.3 Equine Gastric Microbiome

Due to the structure of the gastrointestinal tract horses rely heavily on the symbiotic bacteria that live within the cecum and colon. The site of fermentation is located after the main site of enzymatic breakdown and nutrient absorption (small intestine). Bacteria convert recalcitrant substrates into volatile fatty acids (VFAs), which are readily absorbed with water by the walls of the large intestine. The hybrid design of the digestive tract of the horse depends on the activity of the microbiome to access complex plant material, thus is directly associated with the overall health of the animal.

The first attempt to characterize the microbiome of the horse was in 1975 and the first study to utilize 16S-rRNA sequencing was in 2001.^{7,8} Since then there have been several important taxonomic groups of bacteria that have been identified.⁹ The equine gastric microbiome plays a major role in the overall health of the horse, and provides the horse with approximately 50% of its energy requirements. While the

majority of the microbiome is at home in the hind-gut of the horse, bacterial populations are found throughout the entirety of the gastrointestinal tract.

Two previous studies attempted to characterize the taxonomic composition of the equine stomach and the rest of the gastrointestinal tract.^{9,10} Based on the results of these studies the equine stomach microbiome is comprised of three major phyla, *Firmicutes*, *Proteobacteria*, and *Bacteroidetes*.⁹ Taxa from the phyla *Fusobacteria* and *Actinobacteria* were also present but to a much lesser extent.⁹ Of the taxa belonging to the *Firmicutes* phyla, *Lactobacillus*, *Streptococcus*, and *Sarcina* were the most common species.^{9,10} Of the taxa belonging to the *Proteobacteria* phyla, *Actinobacillus* and *Moraxella* were the most prevalent species.^{9,10} Of the taxa belonging to the *Bacteroidetes* phyla, *Prevotella* and *Porphyromonas* were the most prevalent species. These bacteria are all involved in the breakdown of readily fermentable sugars into lactic acid. Interactions between non steroidal anti-inflammatory drugs in the equine stomach microbiome are not currently well defined. This pilot study seeks to begin making key observations into the interactions between the aforementioned taxa and firocoxib, the newest NSAID approved for use in horses.

As the stomach of the horse is the first organ to see and interact with ingesta, this study looked specifically at the microbiome found in the stomach of the horse and how it interacted with a specific drug treatment. The stomach of the horse is the site of known side effects for this drug treatment and interactions with the microbiome here were of particular interest.

1.4 NSAIDs

Non-steroidal anti-inflammatory drugs are being used more frequently in both human and veterinary medicine because they have similar anti-inflammatory effects of

steroids but are not associated with the long term side effects of steroid use. These drugs are able to reduce inflammation and pain and oftentimes also have antipyretic properties. However there have been deleterious side effects noted with the long term use of NSAID's most notably the formation of gastric ulcers. When looking at these ulcers and their effect on equine health they not only impact the animal's ability to eat they can also have an effect on their behavior due to the pain they cause. Other side effects that have been characterized include right dorsal colitis, which is the inflammation, ulceration, and scarring of the right dorsal colon, and renal papillary necrosis, in which the renal medulla and renal pelvis of the kidney dies.¹¹ There is also evidence that certain classes of NSAIDs, namely COX-2 inhibitors have adverse cardiovascular effects in humans; however these effects have not been characterized in horses.^{12,13}

1.5 What is COX Inhibition?

In order to understand COX inhibition and the associated side effects of inhibiting this enzyme, it is necessary to explain how the normal enzymatic cascade would proceed. Phospholipids are released from cell membranes and are subsequently degraded into arachadonic acid. This product can then be acted upon by the cyclo-oxygenase enzymes to produce prostaglandins and thromboxanes. The ringed products are involved in several other protein cascades that are responsible for homeostatic processes such as mucous production as well as vasoconstriction and vasodialation.^{14,15} The COX-1 enzyme products are directly involved in GI protection via the regulation of the production of mucous and stomach acid, the regulation of blood flow, renal function, and indirectly inflammation, pain, and fever. COX-2

enzyme products, on the other hand, are directly involved in the immune response and directly cause inflammation, pain and fever.

1.5.1 Firocoxib/Equioxx

Horses can be affected by various injuries or chronic conditions that frequently cause pain and inflammation that ultimately impact their performance. Many horse owners routinely administer Nonsteroidal Anti-Inflammatory Drugs (NSAIDs) to reduce the pain and inflammation that is commonly associated with injuries, muscle strains and tears, or chronic conditions such as osteoarthritis. NSAIDs are given frequently with a wide variation in dosage and frequency. Also known as Equioxx; firocoxib was adapted for use in horses from a canine product by the name of Prevacox. ¹⁶⁻²⁰ It is considered to be a second generation NSAID and it is highly selective COX-2 inhibitor, with a COX-1/COX-2 ratio of 268/643. ²¹ It is unlike other NSAIDs on the market because it retains its ability to selectively inhibit COX-2 even at high dosages. ^{24, 25} It is used mainly to treat lameness and other types of orthopedic inflammation, much like phenylbutazone. Horses respond very well to the product, ^{17,19,24} The recommended dosage of firocoxib is .09mg/kg every 24 hours when given intravenously, and .1mg/kg every 24 hours for the paste/oral formulation. ²⁵ There have not been any serious side effects characterized with the long term use of firocoxib other than the normal symptoms of NSAID toxicity and renal damage, namely renal papillary necrosis. ^{16,18-21,26,27} Renal damage is associated with the inhibition of the COX-1 and COX-2 isoforms that help regulate the homeostasis of the kidneys. This disruption in the hormone cascade can in turn cause renal papillary necrosis, a disease where the renal medulla and renal pelvis become necrotic, eventually causing renal failure. ¹¹

Chapter 2

Methods

2.1 Experimental Setup

This study sought to explore the effects of different doses of firocoxib on the gastric microbiome using an in vitro forty-eight hour time-course. The experimental setup for this study involved calculating the correct dosage of firocoxib that would be inoculated, the gastric sample collection and preparation, and the time-course preparation.

2.1.1 Time-course Preparation

This study sought to mimic the equine gastric environment. Anaerobic media was made in order to simulate the contents of the equine stomach. Every liter of anaerobic media contained nutrients, amino acids, volatile fatty acids, and a mixture of acids, buffers, and bases in order to sustain the bacterial populations that were to be introduced to the environment, see Appendix A for full protocol. Ingredients for the media were combined in a 1000mL Erlenmeyer flask that was boiling gently. The Hungate system was used to bubble carbon dioxide through the media mixture in order to ensure that it remained anaerobic. Once the media was mixed, anaerobic, and confirmed to have a pH of 7 it was transferred into 75mL serum vials with Hungate lines placed in all of the vials to keep the media anaerobic. In order to ensure that all changes in pH were due to bacterial activity a pH of 7 was maintained. 64 mL of the media was placed into each serum bottle using an electronic pipetter and the vials

were sealed using blue rubber stoppers. Once all of the media was in its respective container the vials were autoclaved in a custom press to ensure they remained sealed throughout the process and to remove any bacterial contamination. The vials were allowed to cool and then were placed into an incubator set at 39 °C which is the average body temperature of a horse. After sterilization the vials were moved from the incubator to an anaerobic chamber where they were inoculated with 10mL of gastric fluid. Completed vials were removed from the anaerobic chamber and sealed with clamp on aluminum caps. After being sealed the vials were finally inoculated with the firocoxib drug suspension or sterile water via 20G needles according to their respective designations and kept in the incubator when sampling was not actively taking place.

This experiment was conducted in triplicate in order to ensure accuracy within sampling technique and with the results. Low, Medium, and High dosages were represented with three serum vials for a total of nine vials. There were three control vials and three uninoculated vials with low, medium and high dosages of the drug. 1.5mL micro-centrifuge tubes were sterilized using an autoclave and then labeled prior to sampling in order to streamline the process and collected 5mL samples from each serum bottle for each time-point and separated into three 1.5mL micro-centrifuge tubes. Samples were collected using individually packaged, sterile 5mL syringes and 20G needles. See Figure 1 for a visual representation of the experimental set up.

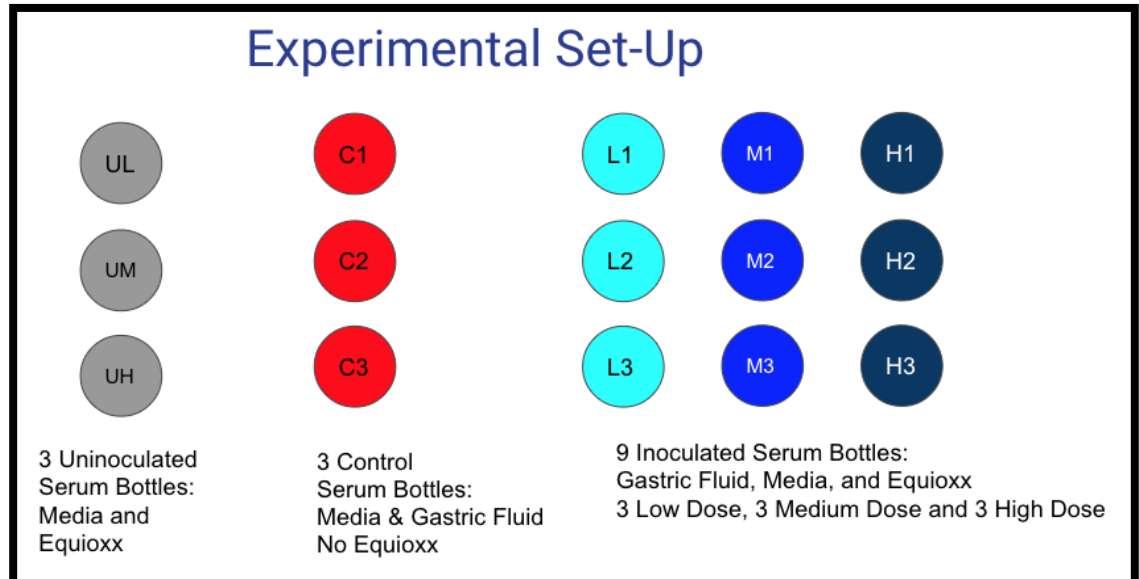


Figure 1: Experimental Set Up

2.1.2 Dosage Calculation

Firocoxib is a newer NSAID that has been approved for use in horses. This study looked into three different doses of firocoxib that were physiologically relevant. The low dose was one half of the recommended dose or .05mg/kg, the medium a full dose or .1mg/kg, and the high was one and a half of the recommended dose or .15mg/kg. Equioxx in a paste formulation was and procured for the study by a licensed veterinarian. The experiment was completed in vitro, as a scaled down model of the equine stomach contained in serum bottle. The doses of firocoxib were calculated and also scaled down to fit the serum bottle model.

The average volume of a horse stomach is twelve liters²⁸. The serum vials used for the study had a volume of 75 mL. The recommended dose of firocoxib as read on the box is .1mg of paste for every kg of horse and there is .0082g of active firocoxib in

every gram of paste.²⁹ The low dose of firocoxib for this study was one half of a recommended dose or .05mg/kg.

Assuming that the average horse is 1000lbs and the average horse stomach is twelve Liters

$$\left(\frac{.05mg}{1kg}\right)\left(\frac{454kg}{12000mL}\right) = 1.89 * 10^{-3} mg/mL$$

$$\left(\frac{1.89 * 10^{-3}mg}{mL}\right)\left(\frac{100 mg}{.82mg}\right)(12000mL) = 2.765g \text{ of paste to normal horse}$$

Assume 75mL stomach:

$$\left(\frac{1.89 * 10^{-3}mg}{mL}\right)(75mL) = 0.14175mg$$

To make suspension in 50mL falcon tube:

$$.14175mg * 50mL = 7.0875mg \frac{\text{paste}}{50mL}$$

The medium dose for this study was the actual recommended dose written on the Equioxx paste package of .1mg/kg. Assuming that the average horse is 1000lbs and the average horse stomach is twelve Liters

$$\left(\frac{.1mg}{1kg}\right)\left(\frac{454kg}{12000mL}\right) = 3.78 * 10^{-3} mg/mL$$

$$\left(\frac{3.78 * 10^{-3}mg}{mL}\right)\left(\frac{100 mg}{.82mg}\right)(12000mL) = 5.537g \text{ of paste to normal horse}$$

Assume 75mL stomach:

$$\left(\frac{3.78 * 10^{-3}mg}{mL}\right)(75mL) = 0.2835mg$$

To make suspension in 50mL falcon tube:

$$.2835mg * 50mL = 14.175mg \frac{paste}{50mL}$$

The high dose for this study was one and a half of the recommended dose or

.15mg/kg. Assuming that the average horse is 1000lbs and the average horse stomach is twelve Liters

$$\left(\frac{.15mg}{1kg}\right)\left(\frac{454kg}{12000mL}\right) = 5.675 * 10^{-3} mg/mL$$

$$\left(\frac{5.675 * 10^{-3}mg}{mL}\right)\left(\frac{100 mg}{.82mg}\right)(12000mL) = 8.304g \text{ of paste to normal horse}$$

Assume 75mL stomach:

$$\left(\frac{5.675 * 10^{-3}mg}{mL}\right)(75mL) = 0.4265mg$$

To make suspension in 50mL falcon tube:

$$.4265mg * 50mL = 21.28125mg \frac{paste}{50mL}$$

To inoculate the serum vials with the Equiox paste, a suspension was created so that

the appropriate amount of drug would be able to be transferred into the appropriate serum vials. The three suspensions were created so that there would be the required dose of drug in 1 ml of the suspension. Each suspension was created with DI water to the total volume of 50 mL. For the low dose, 7.0875mg of the paste was made into a 50 mL suspension; every mL of the low suspension had .14175mg of

firocoxib. The medium dose had 14.175mg of paste made into a 50 mL suspension; every mL of the suspension had 0.2835mg of firocoxib. The high dose had 21.28125mg of paste made into a 50 mL suspension; every mL of the suspension had 0.425mg of firocoxib. Very little of the firocoxib paste went into making these suspensions. The suspensions were made by measuring the appropriate amount of Equioxx paste into the cap of the tube, closing the tube, shaking and vortexing, then adding more DI water to reach 50 mL total volume. Prior to inoculating the serum vials the suspensions were shaken and vortexed thoroughly. The serum vials were inoculated with the appropriate suspension dose using a needle and syringe in order to keep the vials as anaerobic as possible. The inoculation of the serum vials took place once the serum bottle received the gastric fluid and were sealed with the aluminum caps.

2.1.3 Sample Collection

This study utilized gastric fluid samples. Gastric fluid was collected by a veterinarian from a normal, healthy horse at the University of Delaware Webb Farm. The donor horse that was chosen was an adult quarter horse gelding. He was chosen for this study based on his temperament, size, and lack of previous exposure to non-steroidal anti-inflammatory drugs. His lack of previous exposure to NSAIDs was the most important determining factor in his selection for the study as his gastric microbiome can be considered naive to the treatment.

Gastric fluid was collected from the subject by a veterinarian through the use of a nasogastric tube. The materials used for the sample collection process included

the nasogastric tube, a 30 mL syringe, sterile water, collection jar, and two funnels. The water, collection jar, and funnels were sterilized in advance with an autoclave. The nasogastric tube and 30 mL syringe were cleaned on site with ethanol. The nasogastric tube was passed up the nose of the subject and then down his esophagus to reach his stomach, where gastric fluid is located. Using the funnel, sterile water was poured down the tube, then the 30 mL syringe was utilized to create suction with the nasogastric tube to pull up gastric fluid. The gastric fluid was noticeably different than the water as it was green in color and much thicker. When the suction on the nasogastric tube was released, i.e. the removal of the syringe, the gastric fluid was pulled down and out of the tube by gravity. The water came out of the tube first and it was discarded into a bucket. Once the gastric fluid was close to the end of the tube, it was captured and funneled into the prepared sterile collection jar. This process was repeated until approximately 300 mL of gastric fluid was in the collection jar. Once this total was reached, the collection jar was put into a Styrofoam cooler and wrapped in a heating pad to keep it as close to horse body temperature as possible, ~ 39°C, for transportation back to the lab. Upon arrival at the lab, the collection jar of gastric fluid was put into the anaerobic chamber for distribution into the serum vials. Each of the three control serum vials, three low, three medium, and the three high serum vials were inoculated with 10 mL of gastric fluid respectively.

2.2 Experimental Procedure

The complete experimental procedure for this study was made up of several parts including the actual time-course, cell counts, high pressure liquid chromatography, DNA extractions, and quality analysis.

2.2.1 Sampling Procedure

Once all serum vials were inoculated with their respective inoculants, gastric fluid and/or a low, medium or high dosage of firocoxib, the time course could begin. The time course began at 10am with sampling occurring every six hours for forty-eight hours, at 10am, 4pm, 10pm, 4am, et cetera. An additional sampling was done twelve hours after the completion of the time course at hour sixty. When sampling was not taking place, the serum vials were kept in metal trays in an incubator maintained at 39°C, the average body temperature of a horse.

During each sampling time point, the serum vials were removed from the incubator and the tops of each bottle were wiped with ethanol. To measure gas volume, a 20 gauge needle was put onto a 30 mL sterile syringe and inserted into the stopper of the bottle, changing the needle for every bottle. This enables the relief of pressure in the serum bottle and allows the gas volume produced by the bacteria in the bottle to be measured using the markings on the syringe. The gas volume was recorded for all serum vials. Following this measurement, the tops of the vials were again wiped down with ethanol and 20G needles were placed onto 5 mL sterile syringes. For every serum bottle, a 5 mL sample would be drawn and distributed into three 1.5 mL Eppendorf tubes. The pH was tested with litmus paper for each bottle during this step and recorded. After each serum bottle was sampled from, the tops would be wiped down with ethanol, all needles and syringes discarded, and the serum vials taken back to the incubator until the next sampling time point. The Eppendorf tubes containing the sampled material from each of the serum vials were placed in a centrifuge and spun down for 20 minutes at 13,000 RPM. After the centrifuge step, the supernatant of the samples were removed and placed into new 1.5 mL Eppendorf tubes to be utilized for HPLC analysis later on. The pellets left in the original Eppendorf tubes were also

kept for DNA extraction and sequence analysis. All Eppendorf tubes containing the removed supernatant and the spun down pellets were placed into the lab freezer at -20 °C and kept for future analysis after the time course was completed. The above sampling procedure, from gas volume measurement through freezer storage, was repeated at every time point of the study.

2.2.2 Cell Count Procedure

A cell count was performed at the start of the experiment in order to see how many cells were going into the serum vials. 1000 µL of gastric fluid was pipetted into a micro-centrifuge tube and was the stock sample. From there a serial dilution was performed where 10 µL of gastric fluid was added to 90µL of sterile water. This was repeated until the stock solution was diluted 10^{19} times. Samples were loaded into a hemocytometer and counted by two people in order to ensure cell count accuracy. The 10^1 sample in which 10 µL of stock and 90 µL of water were mixed together had the best resolution of cells per square.

2.2.3 HPLC

High performance liquid chromatography, or HPLC, was utilized in this study in order to measure the changes in the metabolites produced by the bacteria through the course of the experiment. HPLC uses a mobile phase, or running buffer, that moves at a specific flow rate. An auto-sampler injects the sample into the mobile phase and the sample and mobile phase move through an HPLC column. The HPLC machine detects and draws peaks when the sample moves through and is separated by the column. Certain metabolites move faster through the column than others, and this is shown by the HPLC output graphs and the peaks that are produced over time. See

Appendix B for complete HPLC protocol. HPLC standards were made, each containing, the desired metabolites at four concentrations for peak assignments and linear regression. Standards one through four contained serial dilutions of glucose, acetate, formate, lactate, and butyrate. Standards five through eight contained serial dilutions of propionate and ethanol. Samples were prepared for HPLC by vortexing the samples, centrifuging for 10 minutes at 13,000 RPM, and filtering with a 0.20 mm syringe filter. Metabolites were measured by HPLC for 30 minutes at 6mL/min using an Aminex column HPX-97H (Biorad). See Appendix B for a detailed list of Standard recipes and the complete HPLC protocol

2.2.4 DNA Extraction

The QIAGEN QIAamp Powerfecal DNA Isolation Kit was used in order to extract bacterial DNA from the samples with the following modifications: Samples A, B, and D from one serum bottle were vortexed, combined, and centrifuged for 10 minutes at 13,000 RPM. The supernatant was then removed and the Bead Solution from the QIAGEN kit added directly to the pellet. Subsequent steps were followed as directed by the instructions in the kit. The QIAGEN kit protocol is comprised of a series of steps that will cause any inorganic material to precipitate out of the sample, lyse bacterial cells, bind DNA, wash out any non-DNA organic matter, and then elute out the bound DNA. See Appendix C for complete QIAGEN QIAamp Powerfecal DNA Isolation Kit instructions. 50µL of concentrated DNA was extracted using the QIAGEN kit.

Before the DNA samples were sent to RTL Genomics for sequencing two quality analysis tests were performed. Nanodrop was used to confirm that DNA was present in the sample to measure the purity of the sample. Qubit measured DNA

concentration in $\mu\text{g/mL}$ by comparing the sample to a set of standards that are made according to Qubit protocol. Once all quality measures were complete for all samples, sample groups A, B, and C were compared to one another and these quality measures were used to determine which group had the best overall purity and concentration of DNA. Samples were shipped to RTL as per their shipping instructions and upon receipt of sequence data further analyses were able to begin.

2.3 Data Analysis

Analysis of the results from the time course data consisted of analyzing gas production, pH, HPLC measurements, DNA sequencing results, as well as statistical tests in R.

2.3.1.1 Gas Production and pH

Gas production and pH data were both measured throughout the time course. Both gas production and pH were measured in triplicate for the control, low, medium, and high serum bottles during the experiment. Triplicate values were averaged for each time-point; this was done separately for the gas production and for the pH data.

2.3.1.2 HPLC Analysis

Following each run of HPLC, each sample was manually integrated and the baselines were all manually adjusted. This manual adjustment process was done by the same person for the all of the HPLC runs in order to maintain consistency. The data for all samples was downloaded from the computer and the peaks were assigned to their specific metabolite. The eight standards contained specific metabolites only and so their peaks were assigned first. The peaks were assigned based on previous Biddle lab data of mean retention times for those metabolites and the shape of their peaks.

Once the standards and their peaks were assigned, the mean retention times for each metabolite were calculated in addition to the standard deviation. The standard deviation of the mean retention times for each metabolite were used to establish an acceptable retention time range that was used to assign peaks for the metabolites in all of the experimental samples. Once peaks were assigned for all samples, remaining unassigned peaks and their data were discarded.

For data analysis, the standards were used to create a standard curve for each metabolite by linear regression. Using the slope and intercept from the standard curves, the concentrations of each of the respective metabolite were calculated for each sample. The formula used to calculate the concentration for each metabolite is as follows: $\text{Concentration} = (\text{Area under curve}) - (\text{intercept}) / \text{slope}$. Following the calculation of concentration for each metabolite for each sample, graphs were created to better visualize the data. Statistics, including a paired t-test and a repeated measures ANOVA were also performed on the data to assess the significance on the variance seen in the samples throughout the time-course.

2.3.1.3 Sequencing Analysis

DNA was sequenced by RTL Genomics in Lubbock, Texas using universal primers for the V4-V5 region of the 16S-rRNA gene. This data was received as FASTQ files. Fast Length Adjustment of Short reads (FLASH) was used to pair forward and reverse sequences together. OIIME 1 (Quantitative Insights Into Microbial Ecology) was used to filter out sequences that are either too short, too long or that do not have enough quality to be accurate. Once the sequences are cleaned up they were assigned sample ID's and were compared to known sequences using the Greengenes reference file. OUT's (Operational Taxonomic Units) were picked with

97% sequence similarity. Using the QIIME biome summarize-table command, the biom file was summarized and count minimum, maximum, mean, median, and standard deviation were found. See Appendix D for further details. Taxa data was summarized into relative abundance and absolute abundance at the genus level (L6) for later statistical analysis. Using L5 relative abundance table, taxa that appeared in less than 50% of the samples were not considered for this study. This sorting enabled a more targeted look into the most prevalent taxa. Once the data was sorted and trimmed, statistical analyses were completed in R.

2.3.1.4 Statistical Testing

Statistical testing done in R utilized the packages DESeq and jamovi. DESeq analyzes count data from high-throughput sequencing assays and tests for differential expression³⁰ whereas jamovi was used to run a nonparametric ANOVA.³¹ R was also used to run a Pearson correlation and to generate heatmaps, Figures 25-30, to display the correlation data.

2.3.1.5 DESeq

DESeq³⁰ was utilized with the L6 absolute abundance data to determine which taxa were differentially abundant between doses of the drug. The following DESeq analyses were run: Control vs. Low vs. Medium vs. High, Control vs. Low, Control vs. Medium, Control vs. High, Low vs. Medium, Low vs. High, and Medium vs. High. The taxa were determined to be significant if their adjusted p-value was less than 0.05.

2.3.1.6 Jamovi ANOVA

Jamovi³¹ was used for non parametric repeated measures ANOVA of relative abundance data across the time-course to determine whether is a package in the R Studio biological statistics package that is able to run a nonparametric ANOVA. This package utilized relative abundance data and compared the changes in the abundance of the bacterial populations across the time course. It was used to determine whether or not the changes seen in the bacterial populations over time were statistically significant. A p value of less than .05 was determined to be statistically significant.

2.3.1.7 Combining HPLC and Sequence Data for Analysis

The Pearson Correlation statistical test compares the linear relationship between two variables. The Pearson correlation test produces a Pearson correlation coefficient as its output. This correlation coefficient ranges from -1 to +1. The closer the output correlation coefficient is to -1 or +1, the stronger the negative or positive correlation is respectively. This test was used to do distinguish which taxa were significantly correlated with the HPLC data for each metabolite. -0.3 and +0.3 were utilized as the cut off values for negative and positive correlations. These values indicate at most a 30% correlation between the two variables and so if the output correlation coefficient is between -0.3 and +0.3, then it can be said there is no correlation between the two variables.

Chapter 3

Results

3.1 Experimental Observations

Experimental observations were made during the time-course at each sampling point. Observations consisted of measurement of gas volume and pH as well as a cell count done prior to the inoculation of the serum vials with gastric fluid. A strong “rotten egg” odor was detected over the entirety of the time-course whenever gas volume measurements were taken.

3.1.1 Gas and pH Data

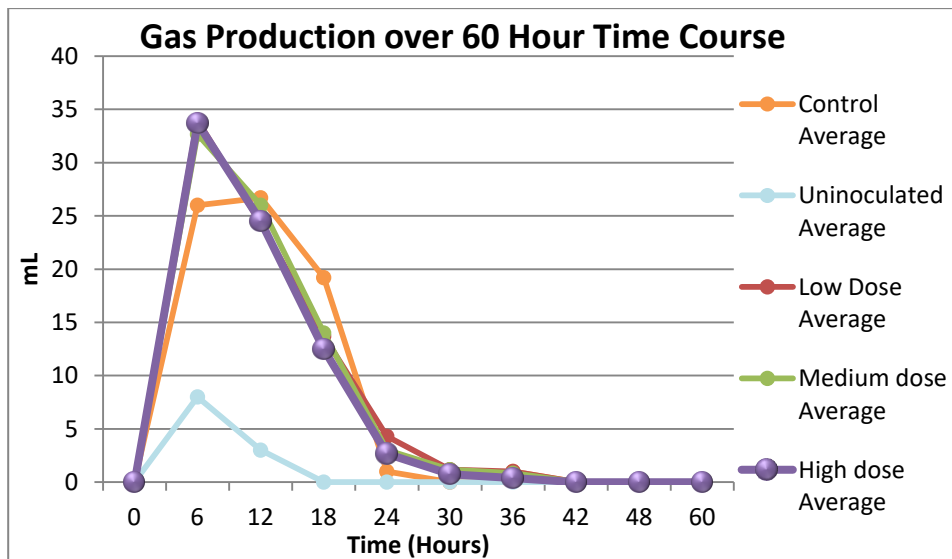


Figure 2: Gas Production over the time-course. Gas produced has a distinct “rotten egg” smell. Serum vials with the same designation were combined

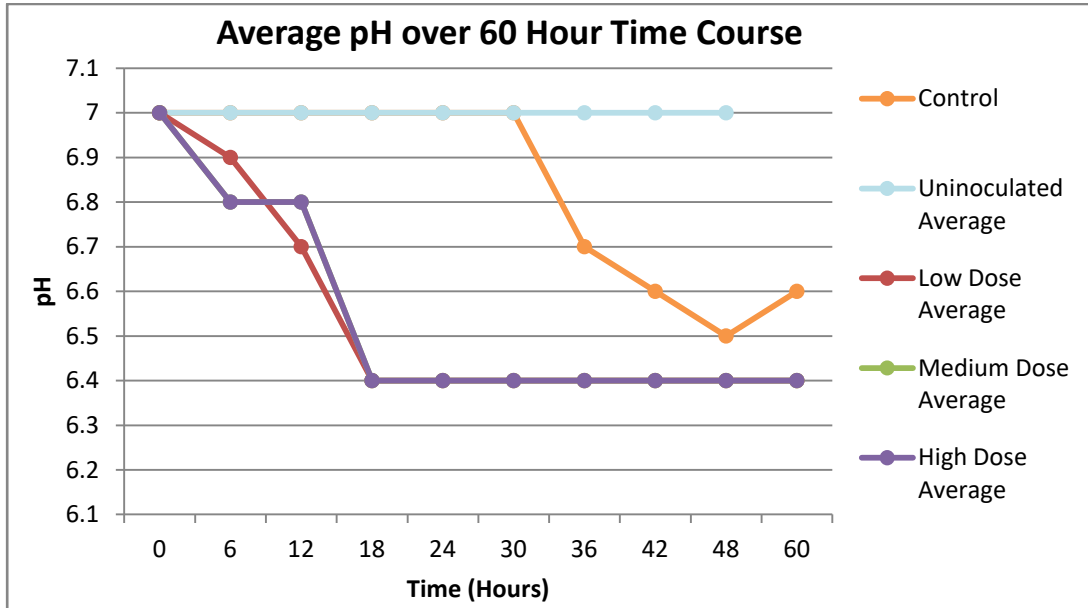


Figure 3: Graphical representation of the pH measurements taken over the time-course. Serum vials with the same designation were combined in order to showcase the average trends.

3.1.2 Cell Count

Cell count data was collected in order to know how many cells were being inoculated into each serum vial.

23	21	25	22
30	39	26	21
S30	32	26	22
23	25	22	30

Figure 4: Mock up of hemocytometer and numbers of cells counted per square. Total number of cells counted was 417. Average number of cells per square is the total divided by the number of squares, which was 16.

$$\frac{N_c * 10^3}{\frac{1}{20} * \frac{1}{20} * \frac{1}{50} * \frac{1}{D}}$$

Where N_c is equal to the average number of cells per square and $1/D$ is equal to the dilution loaded into the hemocytometer. The final cell count for each bottle is shown below.

$$\begin{aligned} &= \frac{26.0625 * 10^3}{\frac{1}{20} * \frac{1}{20} * \frac{1}{50} * \frac{1}{10^1}} \\ &= 5.2125 * \frac{10^7 \text{ cells}}{\text{mL}} * 10 \text{ mL/bottle} \\ &= 5.2125 * 10^8 \text{ cells/bottle} \end{aligned}$$

3.2 HPLC

HPLC data was analyzed using Excel. The concentrations of the metabolites were found using the linear regression of a standard curve based on the data from the known metabolite concentrations in the standards. Each metabolite graph is showcased below.

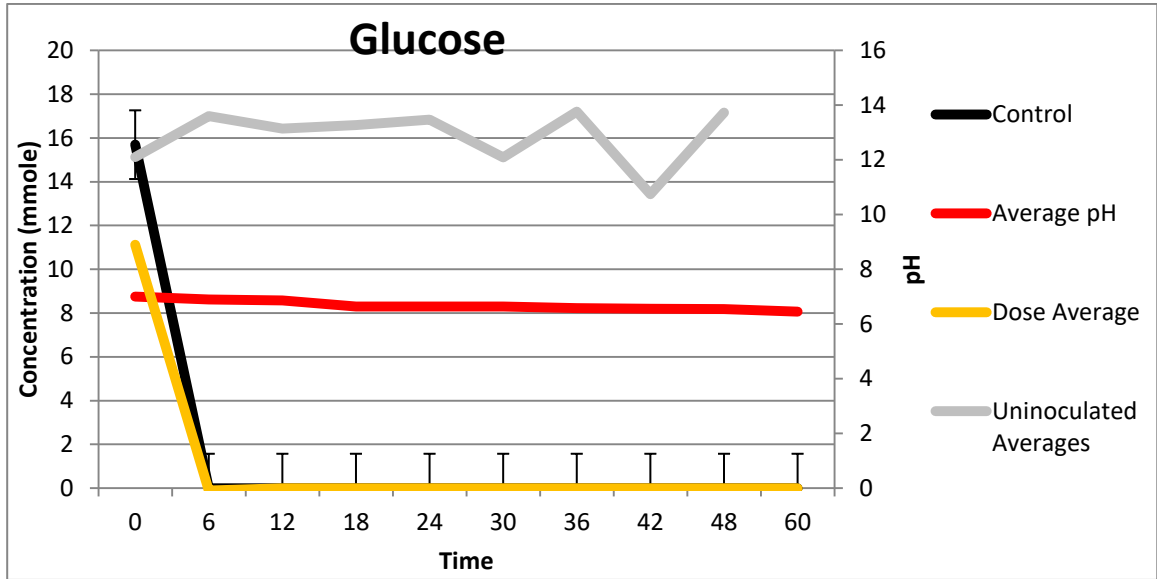


Figure 5: Glucose Production. Dose data was averaged after statistical analysis showing no significant difference between treatments. Average pH data was superimposed on the right axis.

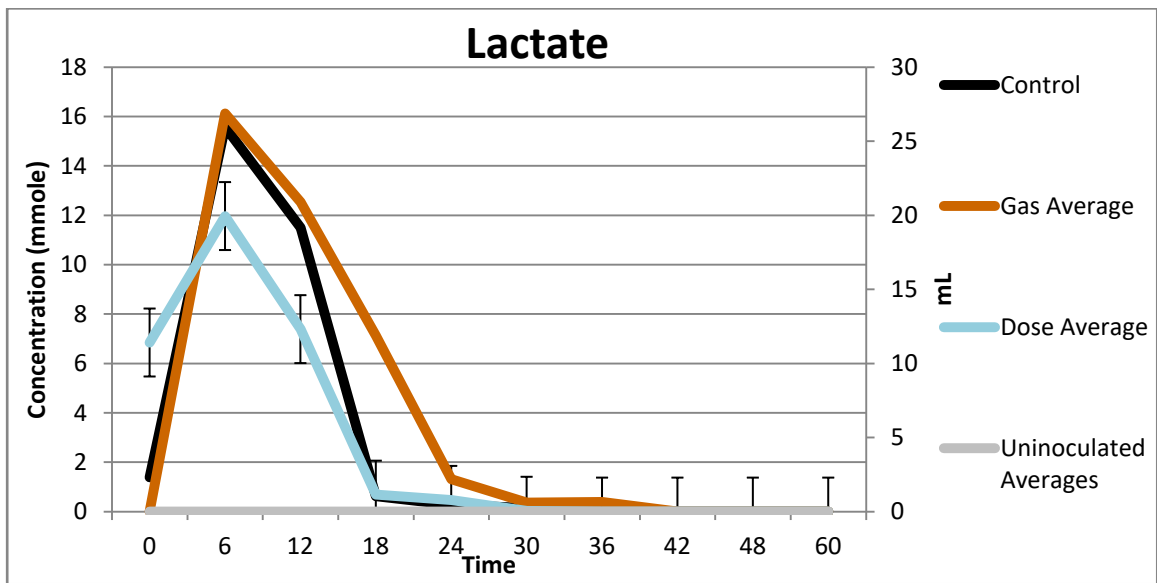


Figure 6: Lactate Production. Dose data was averaged after statistical analysis showing no significant difference between treatments. Average gas volume data was superimposed on the right axis.

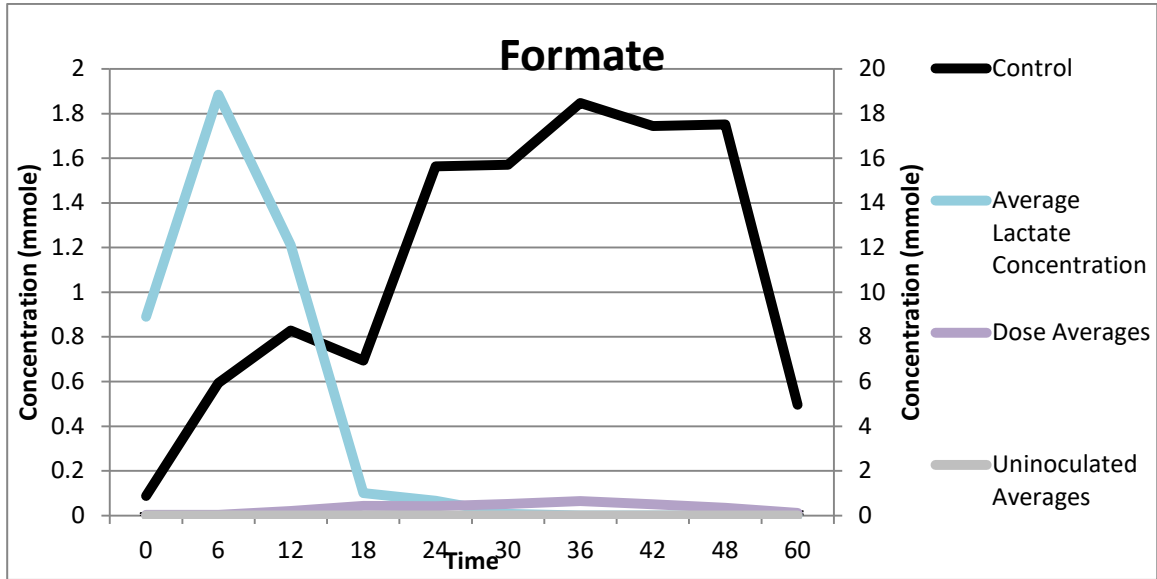


Figure 7: Formate Production. Dose data was averaged after statistical analysis showing no significant difference between treatments. Lactate production was superimposed on the right axis.

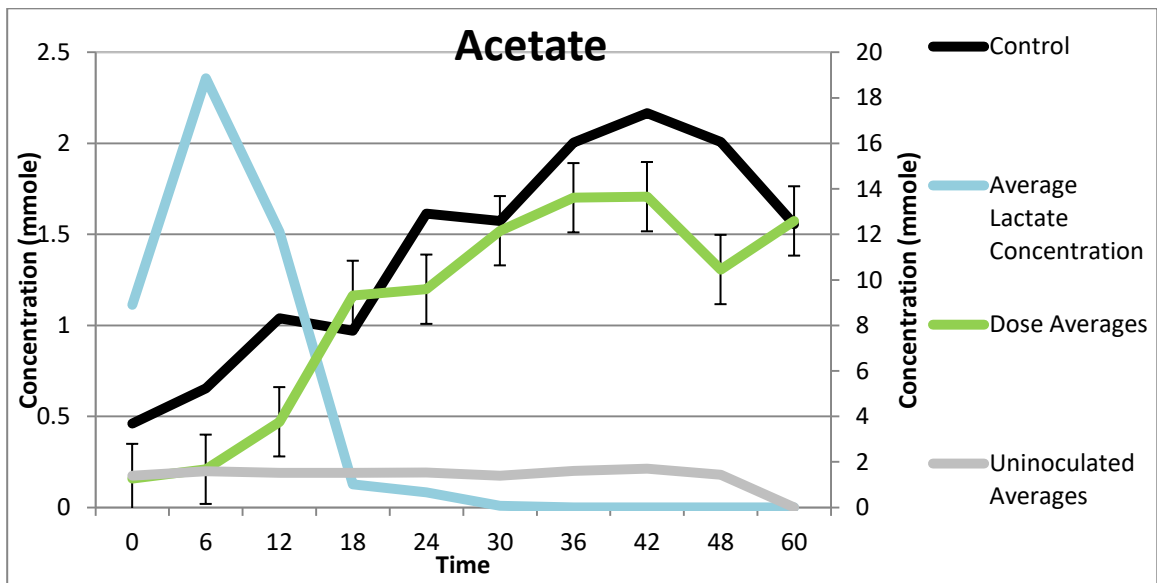


Figure 8: Acetate Production. Dose data was averaged after statistical analysis showing no significant difference between treatments. Lactate production was superimposed on the right axis.

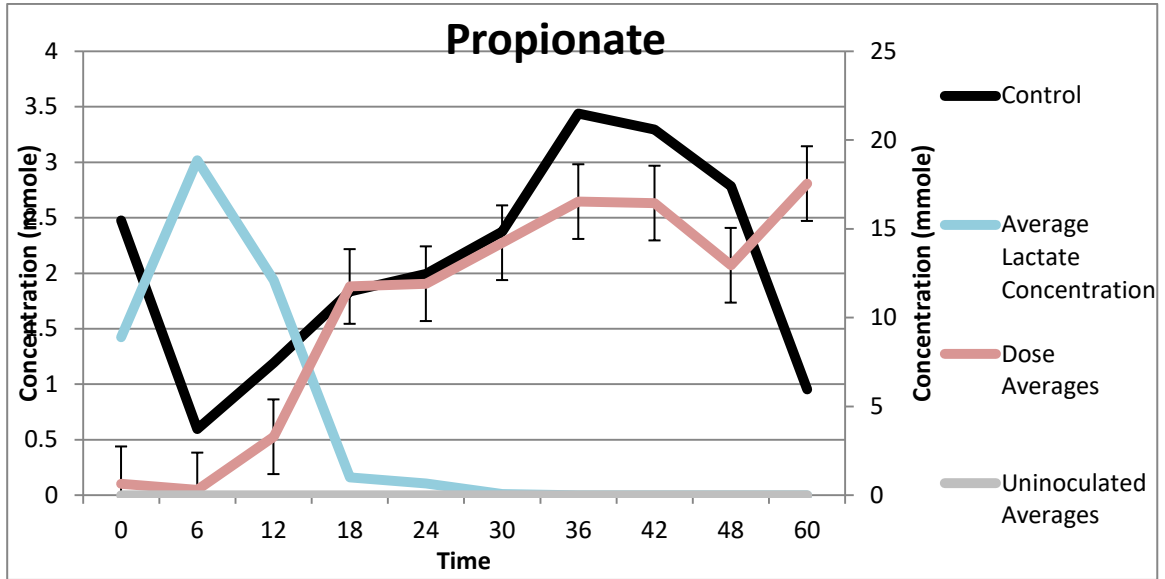


Figure 9: Propionate Production. Dose data was averaged after statistical analysis showing no significant difference between treatments. Lactate production was superimposed on the right axis.

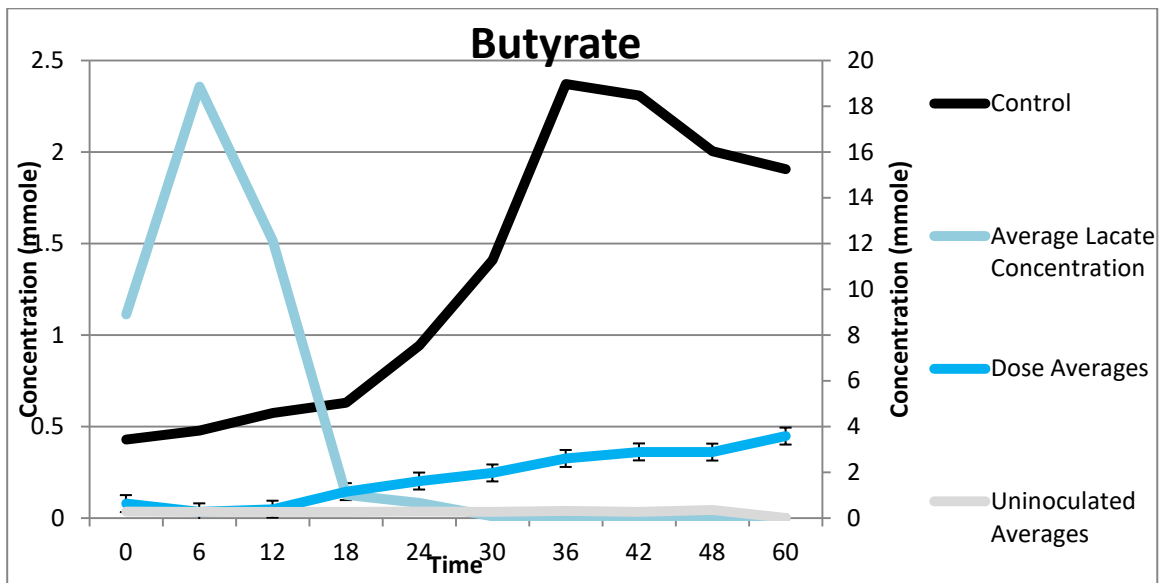


Figure 10: Butyrate Production. Dose data was averaged after statistical analysis showing no significant difference between treatments. Lactate production was superimposed on the right axis.

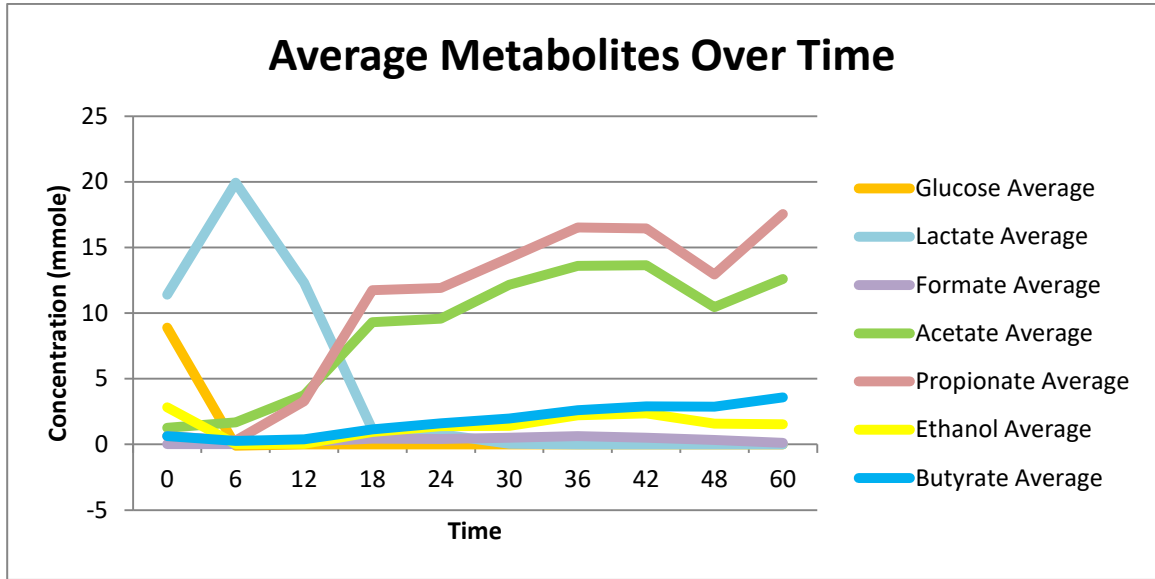


Figure 11: Average metabolites trends over the time-course.

Statistical testing in the form a paired t-test was performed on the data in order to see if there was any significance difference between the three treatment groups. No significant differences were observed in any of the metabolites.

Table 1: Results of the paired t-test illustrating the values that were compared to a p-value of 0.05. Statistically significant differences were highlighted. Missing time-points did not have any detected metabolite concentrations and were excluded from the table.

Metabolite	Time	Low To Medium	Low to High	Medium to High
Glucose	0	0.187027906	0.187499784	0.186865917
	6	0.422649731	0.422649731	0.422649731
Lactate	0	0.630950162	0.414059289	0.421138263
	6	0.709721315	0.552693275	0.521714763
	12	0.65868855	0.470587237	0.339176488
	18	0.771601129	0.185403537	0.186093473
	24	0.035870626	0.970523803	0.052490915
	30	0.346351004	0.346351004	-
Formate	0	0.432342013	0.739167126	0.382965755

	6	0.422649731	0.422649731	0.422649731
	12	0.286581842	0.305379643	0.581084468
	18	0.232828841	0.694971398	0.701054755
	24	0.100796336	0.190127647	0.089420312
	30	0.856582646	0.692287241	0.493419922
	36	0.087610152	0.511051857	0.236603554
	42	0.085409403	0.005646191	0.228093878
	48	0.964712345	0.786279984	0.685970119
	60	0.82715513	0.419184243	0.537280292
Acetate	0	0.403084339	0.307358162	0.370945714
	6	0.741815543	0.186150071	0.181919094
	12	0.276637529	0.212474016	0.286435588
	18	0.12007005	0.846973381	0.748856025
	24	0.316752678	0.833210705	0.391513975
	30	0.901221344	0.745140007	0.653837948
	36	0.279694022	0.29048037	0.251240695
	42	0.420201694	0.104272384	0.321995467
	48	0.612424473	0.483000026	0.482746603
	60	0.495982148	0.641678244	0.336697448

Metabolite	Time	Low To Medium	Low to High	Medium to High
Propionate	0	0.426857249	0.406909411	0.252714202
	6	0.841728217	0.279414566	0.258741507
	12	0.282803994	0.208727598	0.213956884
	18	0.077870703	0.886450018	0.800470386
	24	0.17649849	0.984364613	0.298161986
	30	0.703574063	0.972250873	0.55496653
	36	0.318306357	0.474644541	0.294281831
	42	0.705396952	0.415138682	0.46159656
	48	0.615099402	0.464891445	0.439646004
	60	0.23871076	0.839546257	0.153214359
Butyrate	0	0.376189606	0.772234581	0.403266772
	6	0.948929491	0.096589905	0.247432074
	12	0.292942606	0.251559948	0.28733272
	18	0.732654	0.373504426	0.185661202
	24	0.179836094	0.797298104	0.326189161
	30	0.664072181	0.94873161	0.5665609
	36	0.329068626	0.847500253	0.365479098
	42	0.54533006	0.971345987	0.585133553
	48	0.298567698	0.264206444	0.835244748
	60	0.112108676	0.849177301	0.248812907

3.3 16S-rRNA Sequence Data and QIIME

The biom file was summarized and count minimum, maximum, mean, median, and standard deviation were found. The average number of sequences per sample was, 12,859.5 see Appendix D for further detail. Utilizing the relative abundance data from the QIIME analysis there were 43 taxa at the genus level that were found in 50% or more of the samples. These taxa groups were the focus of subsequent analyses and statistical testing. The figure showcases the relative abundance of the 43 taxa and how these abundances changed over the time-course and by treatment.

Table 2: The 43 significant taxa groups are summarized. Taxa with an * were the taxa excluded from Figure 14 due to their relative abundances being less than .01% throughout the entire time-course.

Kingdom	Phyla	Class	Order	Famiy	Genus
Bacteria	Firmicutes	Bacilli	Gemellales	Gemellaceae	Gemella
Bacteria	Firmicutes	Bacilli	Lactobacillales	Other	Other
Bacteria	Firmicutes	Bacilli	Lactobacillales	f__	g__
Bacteria	Firmicutes	Clostridia	Clostridiales	Other	Other
Bacteria	Firmicutes	Clostridia	Clostridiales	f__	g__
Bacteria	Firmicutes	Clostridia	Clostridiales	Clostridiaceae	Clostridium*
Bacteria	Firmicutes	Clostridia	Clostridiales	Lachnospiraceae	Other
Bacteria	Firmicutes	Clostridia	Clostridiales	Lachnospiraceae	g__
Bacteria	Firmicutes	Clostridia	Clostridiales	Lachnospiraceae	Butyrivibrio*
Bacteria	Firmicutes	Clostridia	Clostridiales	Lachnospiraceae	Catonella*
Bacteria	Firmicutes	Clostridia	Clostridiales	Lachnospiraceae	Moryella
Bacteria	Firmicutes	Clostridia	Clostridiales	Lachnospiraceae	Oribacterium
Bacteria	Firmicutes	Clostridia	Clostridiales	Peptostreptococcaceae	Peptostreptococcus *
Bacteria	Firmicutes	Clostridia	Clostridiales	Ruminococcaceae	g__*
Bacteria	Firmicutes	Clostridia	Clostridiales	Veillonellaceae	Other*
Bacteria	Firmicutes	Clostridia	Clostridiales	Veillonellaceae	g__
Bacteria	Firmicutes	Clostridia	Clostridiales	Veillonellaceae	Acidaminococcus
Bacteria	Firmicutes	Clostridia	Clostridiales	Veillonellaceae	Dialister
Bacteria	Firmicutes	Clostridia	Clostridiales	Veillonellaceae	Megasphaera
Bacteria	Firmicutes	Clostridia	Clostridiales	Veillonellaceae	Succinidasticum
Bacteria	Firmicutes	Clostridia	Clostridiales	Veillonellaceae	Veillonella
Bacteria	Firmicutes	Clostridia	Clostridiales	[Mogibacteriaceae]	g__
Bacteria	Proteobacteria	Betaproteobacteria	Burkholderiales	Alcaligenaceae	Sutterella
Bacteria	Proteobacteria	Betaproteobacteria	Neisseriales	Neisseriaceae	Other
Bacteria	Proteobacteria	Gammaproteobacteria	Enterobacteriales	Enterobacteriaceae	Other*
Bacteria	Proteobacteria	Gammaproteobacteria	Enterobacteriales	Enterobacteriaceae	g__
Bacteria	Proteobacteria	Gammaproteobacteria	Enterobacteriales	Enterobacteriaceae	Erwinia
Bacteria	Proteobacteria	Gammaproteobacteria	Pasteurellales	Pasteurellaceae	Other
Bacteria	Proteobacteria	Gammaproteobacteria	Pasteurellales	Pasteurellaceae	Actinobacillus
Bacteria	Proteobacteria	Gammaproteobacteria	Pasteurellales	Pasteurellaceae	Aggregatibacter
Bacteria	Proteobacteria	Gammaproteobacteria	Xanthomonadales	Xanthomonadaceae	g__
Bacteria	Bacteroidetes	Bacteroidia	Bacteroidales	Bacteroidaceae	Bacteroides
Bacteria	Bacteroidetes	Bacteroidia	Bacteroidales	Porphyromonadaceae;	Parabacteroides *
Bacteria	Bacteroidetes	Bacteroidia	Bacteroidales	Prevotellaceae;	Prevotella
Bacteria	Bacteroidetes	Bacteroidia	Bacteroidales	[Paraprevotellaceae]	Other
Bacteria	Bacteroidetes	Bacteroidia	Bacteroidales	[Paraprevotellaceae]	g__
Bacteria	Bacteroidetes	Bacteroidia	Bacteroidales	[Paraprevotellaceae]	CF231
Bacteria	Bacteroidetes	Bacteroidia	Bacteroidales	[Paraprevotellaceae]	[Prevotella]
Bacteria	Fusobacteria	Fusobacteriia	Fusobacteriales	Fusobacteriaceae	Other*
Bacteria	Fusobacteria	Fusobacteriia	Fusobacteriales	Fusobacteriaceae	Fusobacterium
Bacteria	Fusobacteria	Fusobacteriia	Fusobacteriales	Leptotrichiaceae	Leptotrichia
Bacteria	Actinobacteria	Actinobacteria	Bifidobacteriales	Bifidobacteriaceae	g__*
Unassigned	Other	Other	Other	Other	Other

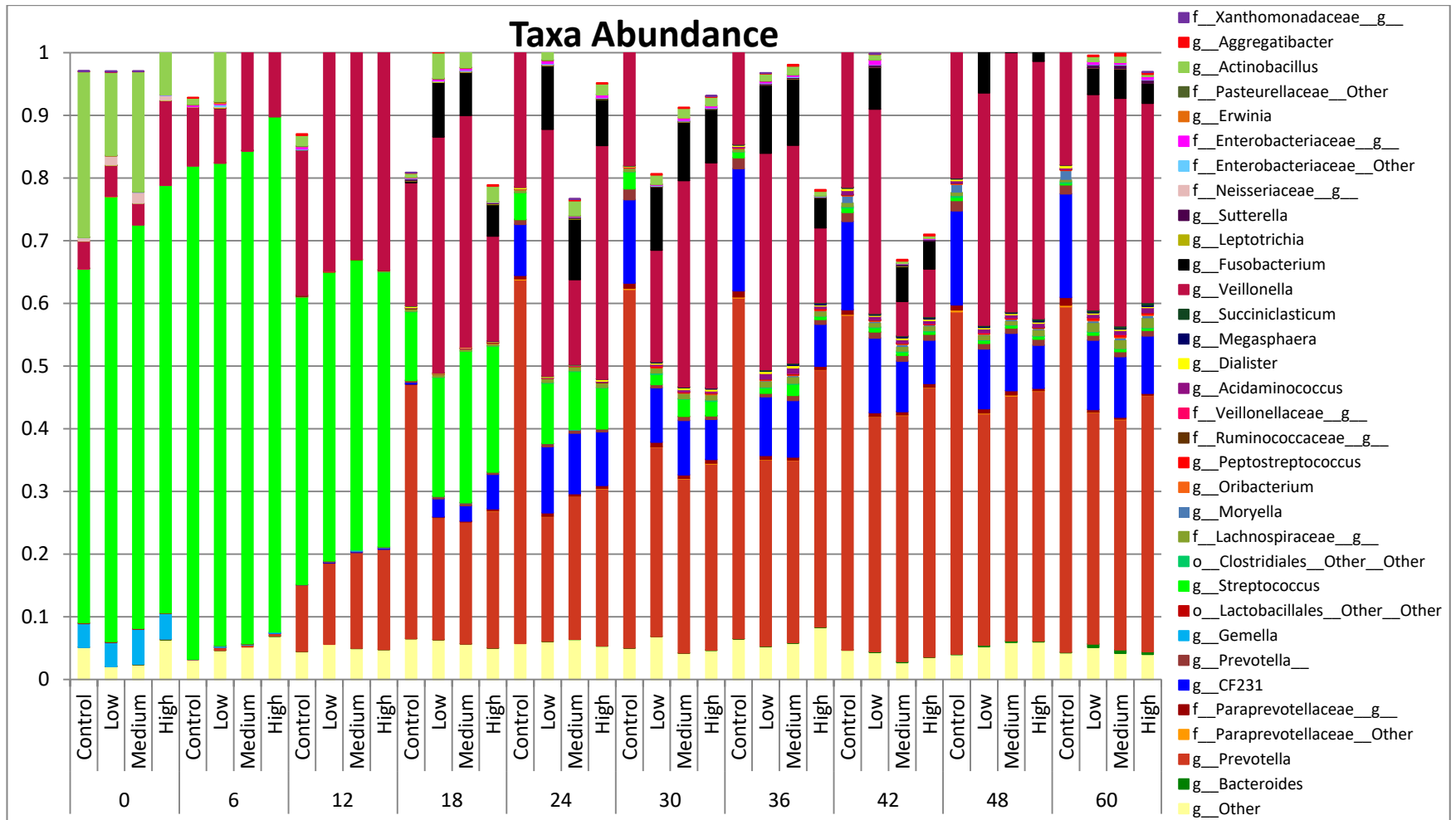


Figure 12: Stacked bar graph illustrating 33 of the 43 important taxa and how their abundances change over the time-course and by treatment.

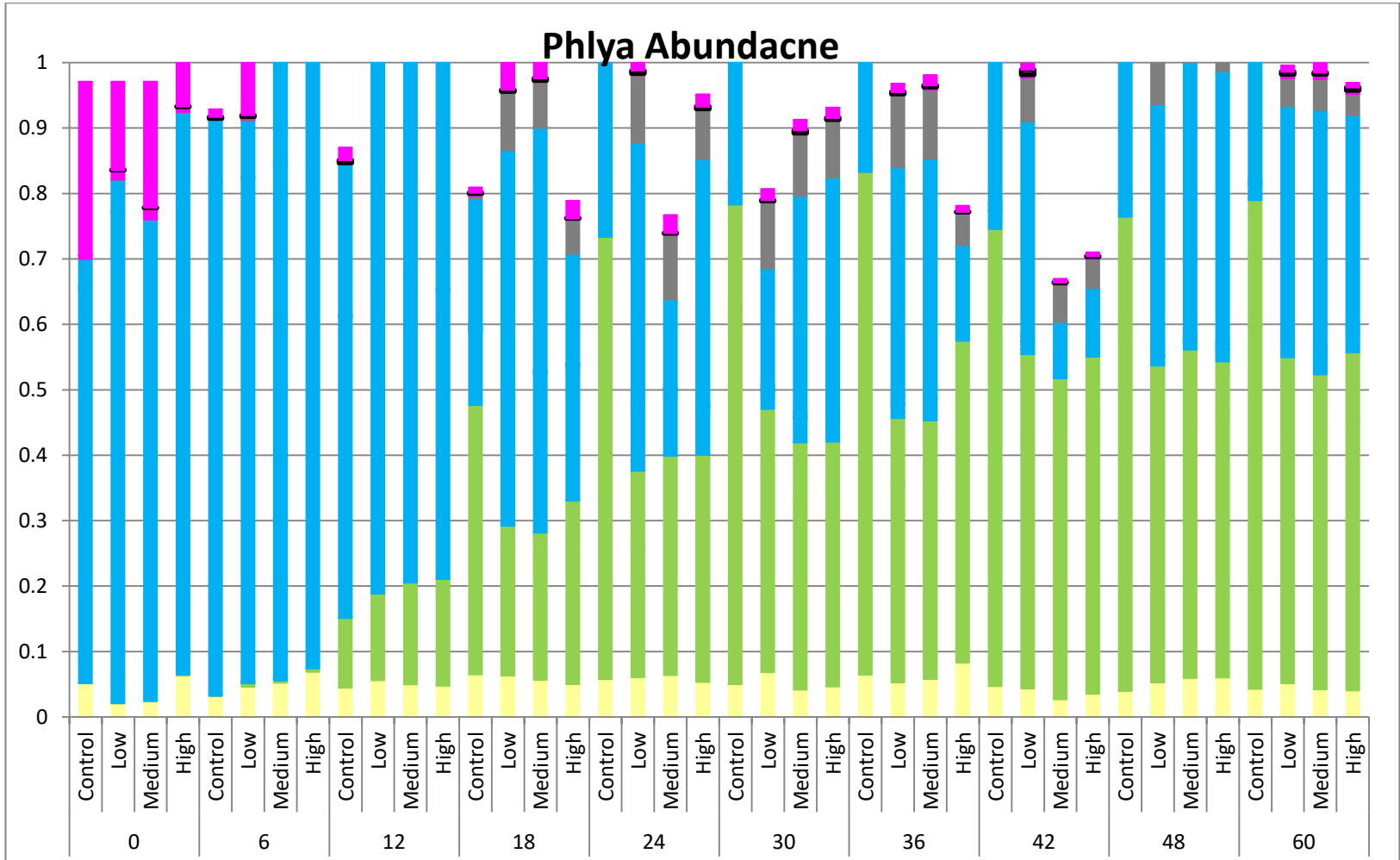


Figure 13: Taxa Abundance by Phyla in which *Other* is pale yellow, *Bacteriodes* is green, *Firmicutes* is bright blue, *Fusobacterium* is gray, and *Proteobacteria* is pink

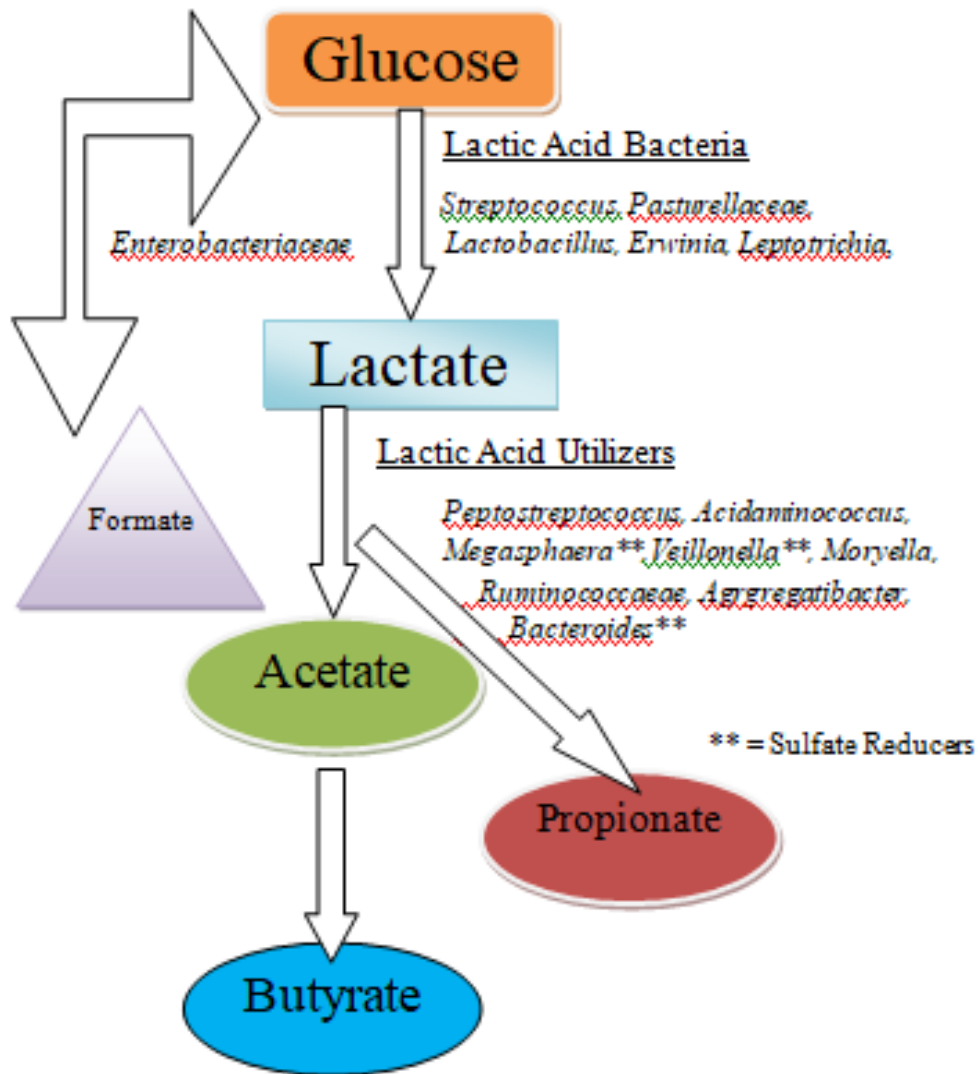


Figure 14: Metabolic pathways of metabolites tracked via HPLC and drug affected taxa.

3.3.1 JAMOVİ

Statistical analysis of the relative abundance data was analyzed in R. The JAMOVİ package is a non-parametric repeated measures Analysis Of Variance (ANOVA). The ANOVA test was used in order to determine if the changes in abundance of the bacteria were due to the change in time or due to treatment. The

absolute abundances of only three of the 43 significant taxa were found to not change significantly over time, *Bifidobacteriaceae*, *Lachnospiraceae*, and *Catonella*.

Unfortunately there was not enough sequence data per time point in order to determine whether or not treatment significantly affected the relative abundance of the bacteria as only one DNA sample per treatment per time point was sent for sequencing.

Table 3: The 43 important taxa and the p-value generated by the JMV ANOVA. p-values less than 0.05 were considered significant. Taxa are colored by phyla according to Figure 2. Taxa with a * were excluded from abundance figures because they had less than .01% abundance throughout the time-course.

Taxa	JMV P -Value
o_Clostridiales_f_g_	0.006
o_Clostridiales_Other_Other	< .001
o_Lactobacillales_Other_Other	< .001
f_Mogibacteriaceae_g_	< .001
f_Pasteurellaceae_Other	0.002
f_Ruminococcaceae_g_	< .001 *
f_Veillonellaceae_g_	< .001
f_Veillonellaceae_Other	0.001
f_Lachnospiraceae_g_	< .001
f_Lachnospiraceae_Other	0.311
f_Neisseriaceae_g_	< .001 *
f_Enterobacteriaceae_g_	< .001
f_Enterobacteriaceae_Other	0.002 *
f_Xanthomonadaceae_g_	< .001
f_Paraprevotellaceae_g_	< .001
f_Paraprevotellaceae_Other	< .001
f_Fusobacteriaceae_Other	0.002 *
f_Bifidobacteriaceae_g_	0.517 *

Table 4: 43 important taxa as well as the p-value generated by the JMV ANOVA. p-values less than 0.05 were considered significant. Taxa are colored by phyla according to Figure 2. Taxa with a * were excluded from abundance figures because they had less than .01% abundance throughout the time-course.

Taxa	JMV P -Value
g__Acidaminococcus	< .001
g__Butyrivibrio	< .001 *
g__Catonella	0.08
g__Clostridium	0.008 *
g__Dialister	< .001
g__Veillonella	< .001
g__Megasphaera	< .001
g__Moryella	< .001
g__Oribacterium	< .001
g__Peptostreptococcus	< .001 *
g__Gemella	< .001
g__Succinoclasticum	< .001
g__Streptococcus	< .001
g__Catenibacterium	< .001
g__Actinobacillus	< .001
g__Aggregatibacter	< .001
g__Sutterella	< .001
g__Erwinia	< .001
g__Bacteroides	< .001
g__CF231	< .001
g__Prevotella	< .001
g__Prevotella__	< .001
g__Fusobacterium	< .001
g__Leptotrichia	< .001
g__Porphyromonas	0.009
g__Other	0.006

3.3.2 DESeq

Since the JMV ANOVA was unable to take into account any possible dose effect on the relative abundances of the bacteria populations, the R DESeq package was used in order to see if there was a dose effect on the abundances of the bacteria.

Table 5: Taxa groups whose absolute abundances were significantly affected by dose.

Comparison	Taxa	Adjusted P-Value
All	g_Fusobacterium	0.006867989
	f_Enterobacteriaceae__Other	0.014039821
	g_Actinobacillus	0.049705577
Control_High	g_Other	1.70E-06
	g_Prevotella	0.037843211
	f_Paraprevotellaceae__Other	0.002812751
	g_Prevotella__	0.033336467
	o_Clostridiales__Other__Other__	0.036995739
	g_Moryella	0.011163849
	g_Fusobacterium	9.84E-05
	g_Actinobacillus	5.42E-05
	g_Aggregatibacter	0.001635237
Control_Low	g_Other	0.000482946
	g_Parabacteroides	0.036736973
	g_Prevotella	0.036473936
	f_Paraprevotellaceae__Other	0.009071414
	g_Prevotella__	0.036763423
	g_Clostridium	0.046591446
	g_Moryella	0.015367065
	f_Fusobacteriaceae__Other	0.045295229
	f_Enterobacteriaceae__g__	0.011112898
	g_Actinobacillus	0.005787147
	g_Aggregatibacter	0.015221341
Control_Medium	g_Other	0.012070445
	g_Prevotella	0.023345021
	f_Paraprevotellaceae__Other	0.011034734
	g_Prevotella__	0.025976744
	o_Clostridiales__Other__Other	0.024394091
	o_Clostridiales__f__g__	0.04380858
	g_Moryella	0.030337143
	g_Fusobacterium	6.92E-06
	g_Leptotrichia	0.010840841
	f_Enterobacteriaceae__Other	0.023520356
	f_Enterobacteriaceae__g__	0.015949794
	g_Actinobacillus	0.005799383
	g_Aggregatibacter	0.000163994
	Low_High	No significant groups
Low_Medium	o_Lactobacillales__Other__Other	0.010894192
Medium_High	No Significant Groups	-

3.4 Sequence Data and HPLC Correlation

Pearson correlations were measured between the absolute abundances of the significant taxa groups and the metabolites identified by the HPLC.

3.4.1 Positive Correlation

The following figures summarize the taxa that demonstrated a positive correlation across the time-course. 0.3 was the lower limit to indicate a positive correlation.

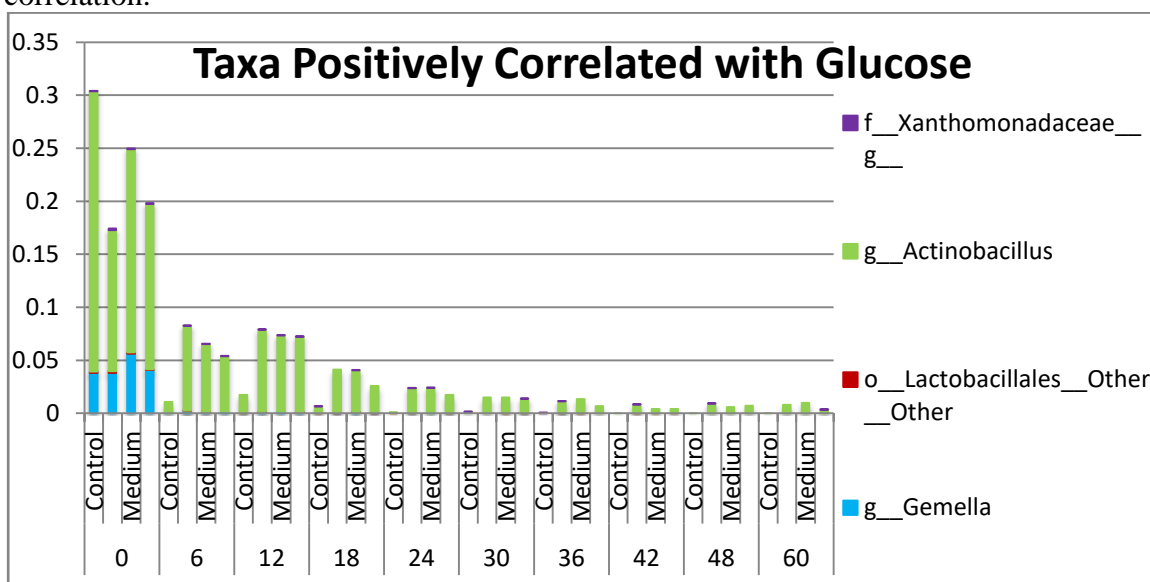


Figure 15: Taxa positively correlated with glucose over the time-course.

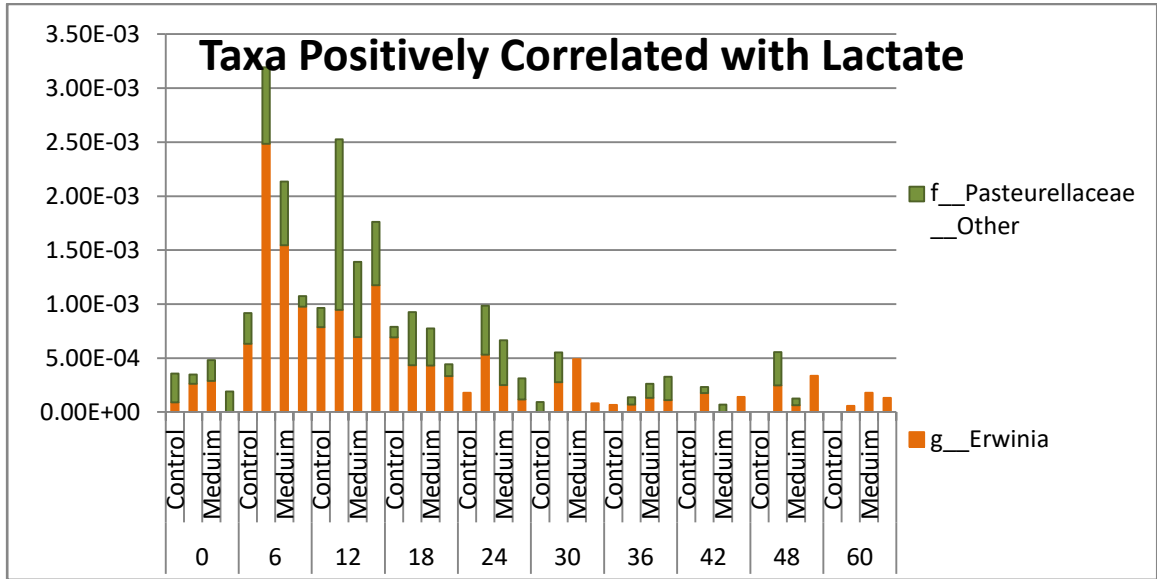


Figure 16: Taxa positively correlated with lactate over the time-course.

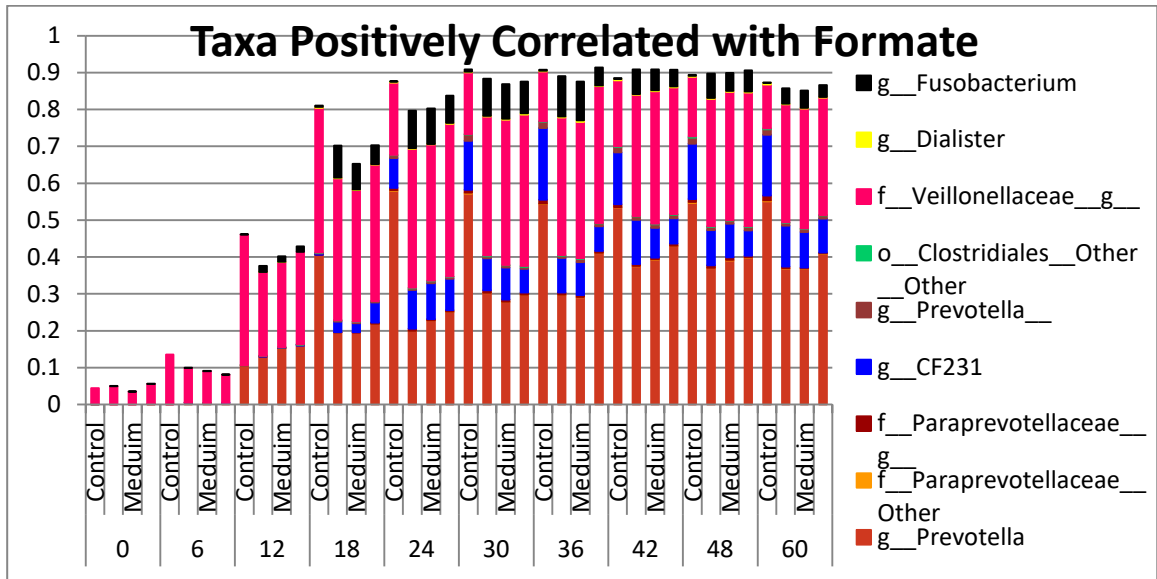


Figure 17: Taxa positively correlated with formate over the time-course.

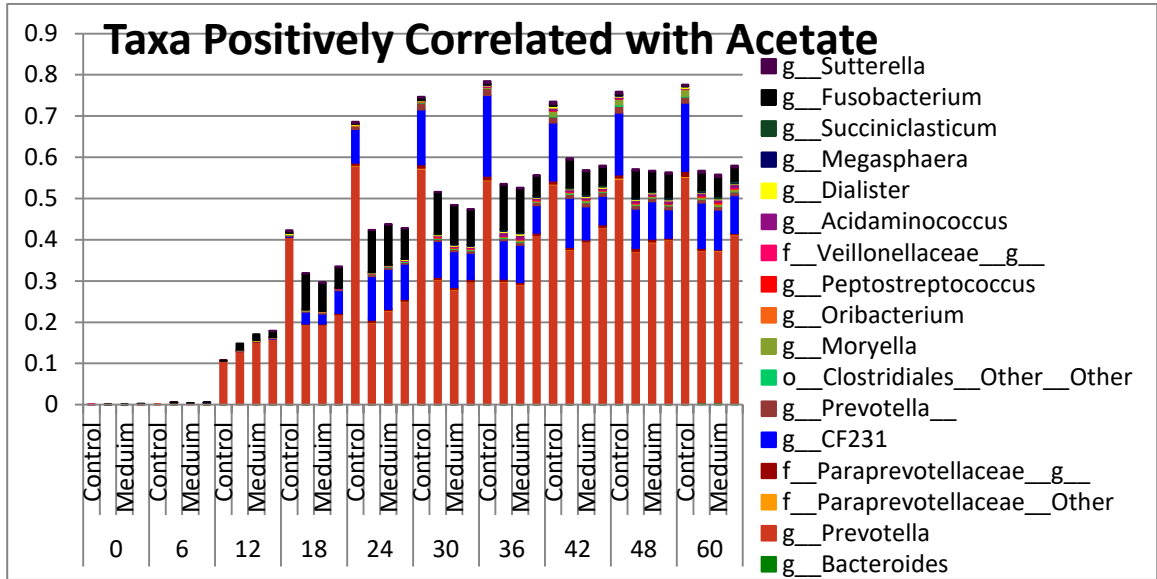


Figure 18: Taxa positively correlated with acetate over the time-course.

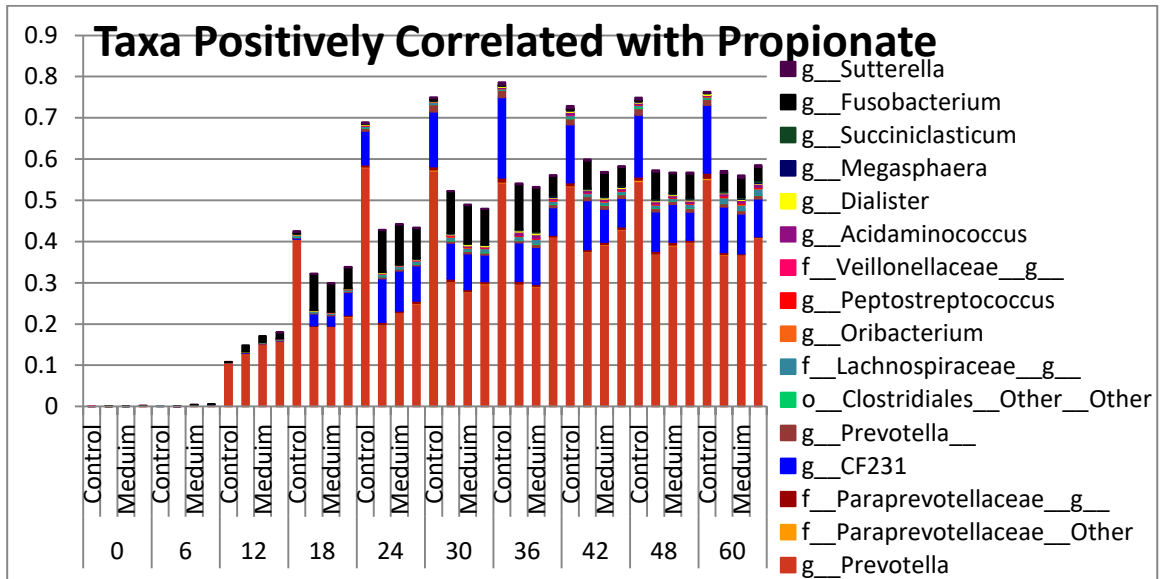


Figure 19: Taxa positively correlated with propionate over the time-course.

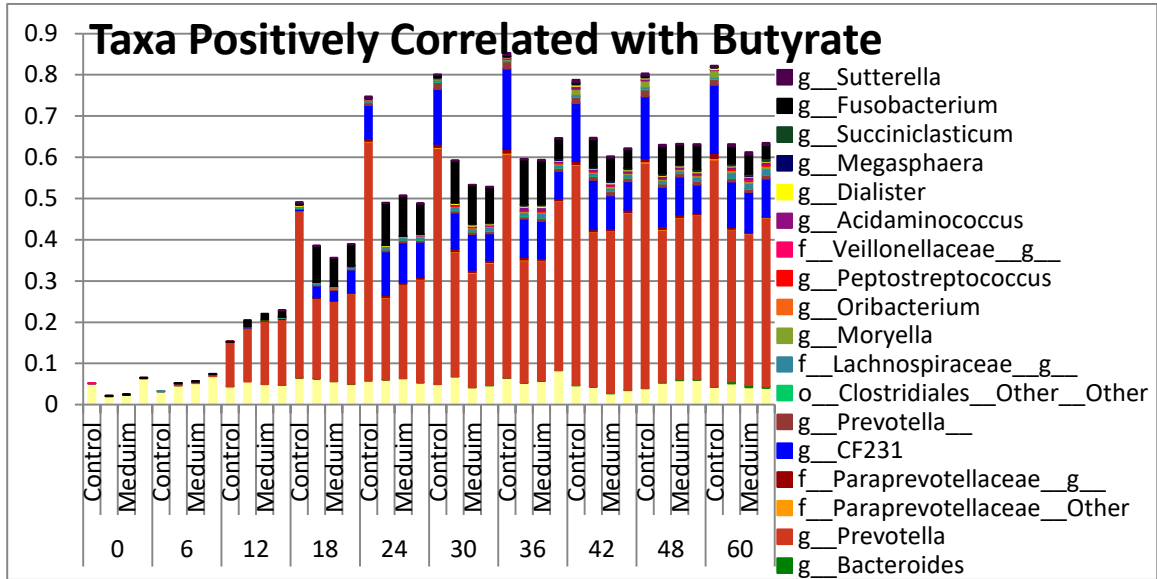


Figure 20: Taxa positively correlated with butyrate over the time-course.

3.4.2 Negative Correlation

The following figures summarize the taxa that demonstrated a positive correlation across the time-course. -0.3 was the upper limit to indicate a negative correlation.

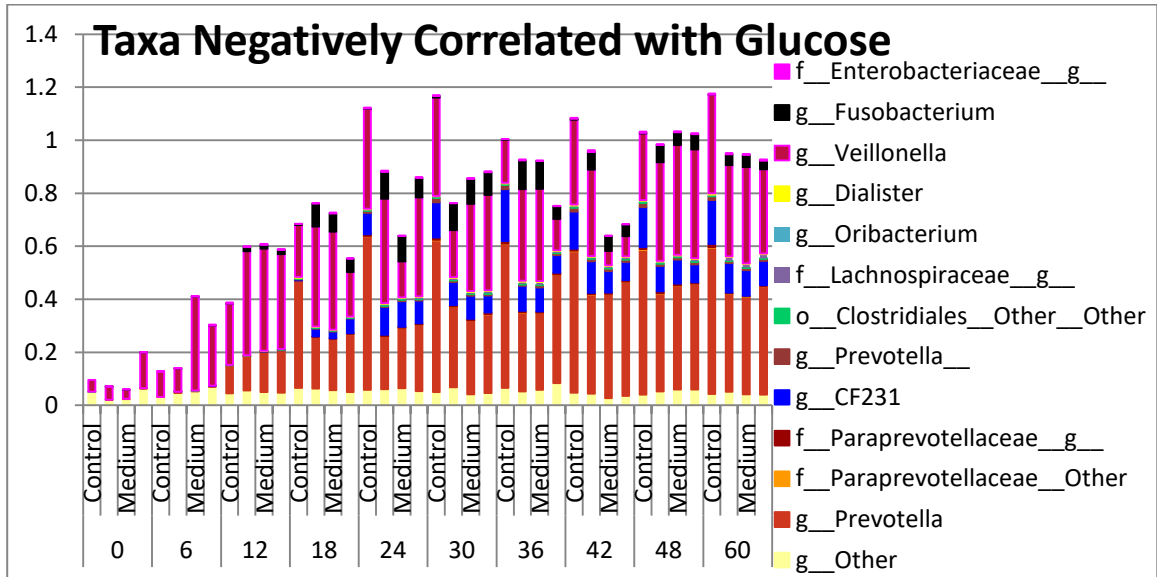


Figure 21: Taxa negatively correlated with glucose over the time-course.

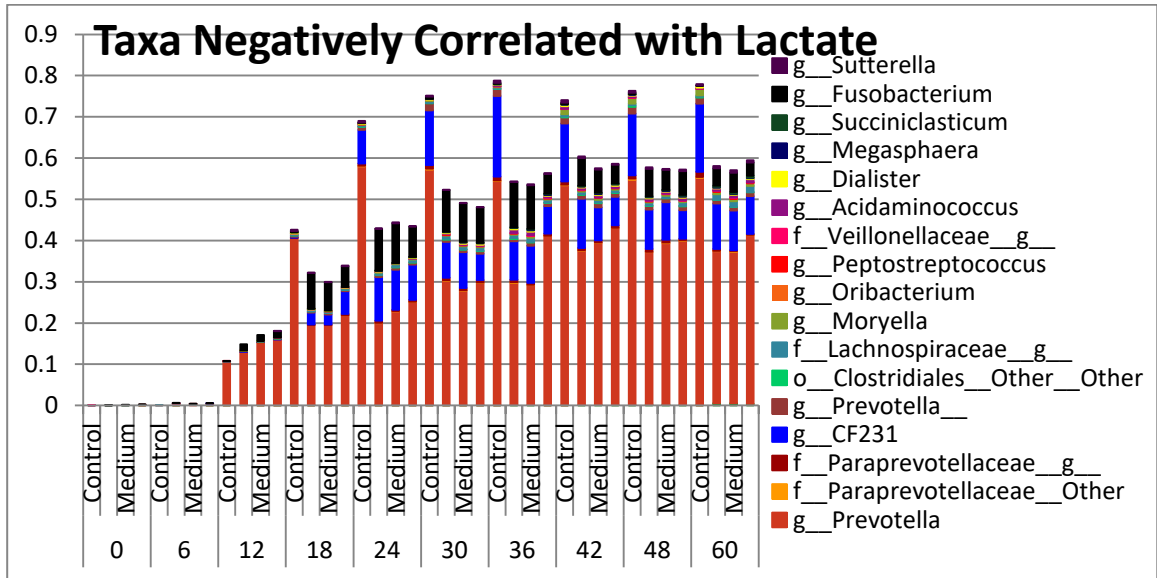


Figure 22: Taxa negatively correlated with lactate over the time-course.

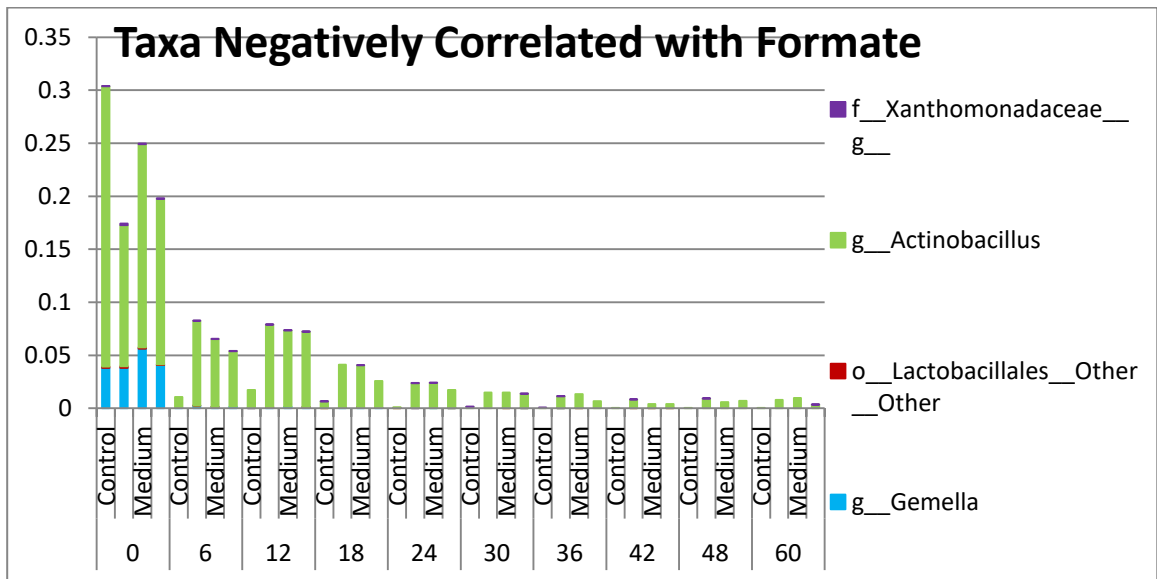


Figure 23: Taxa negatively correlated with formate over the time-course.

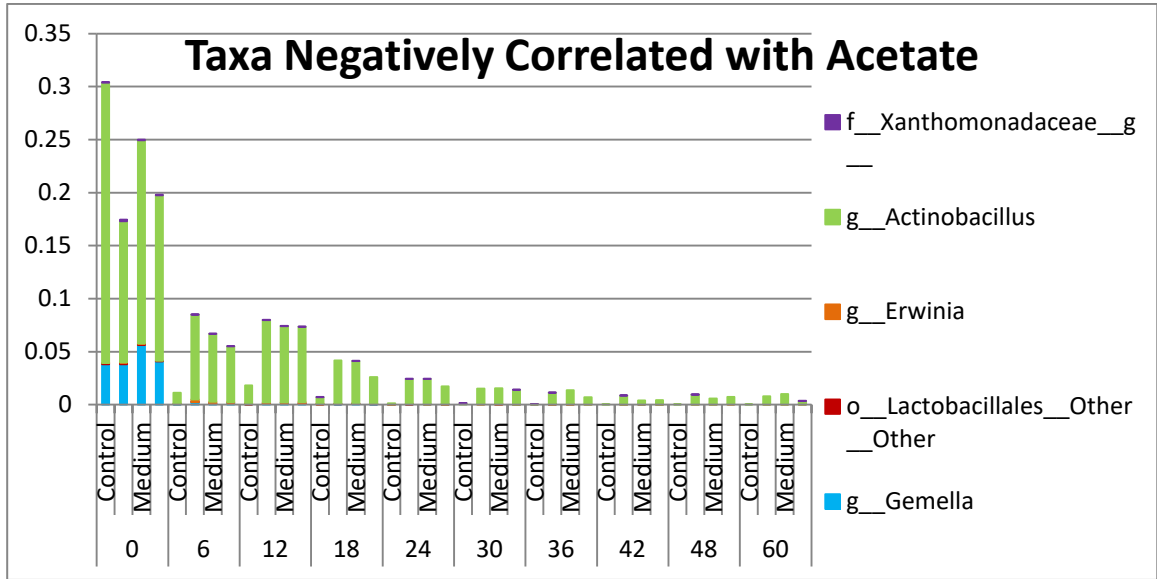


Figure 24: Taxa negatively correlated with acetate over the time-course.

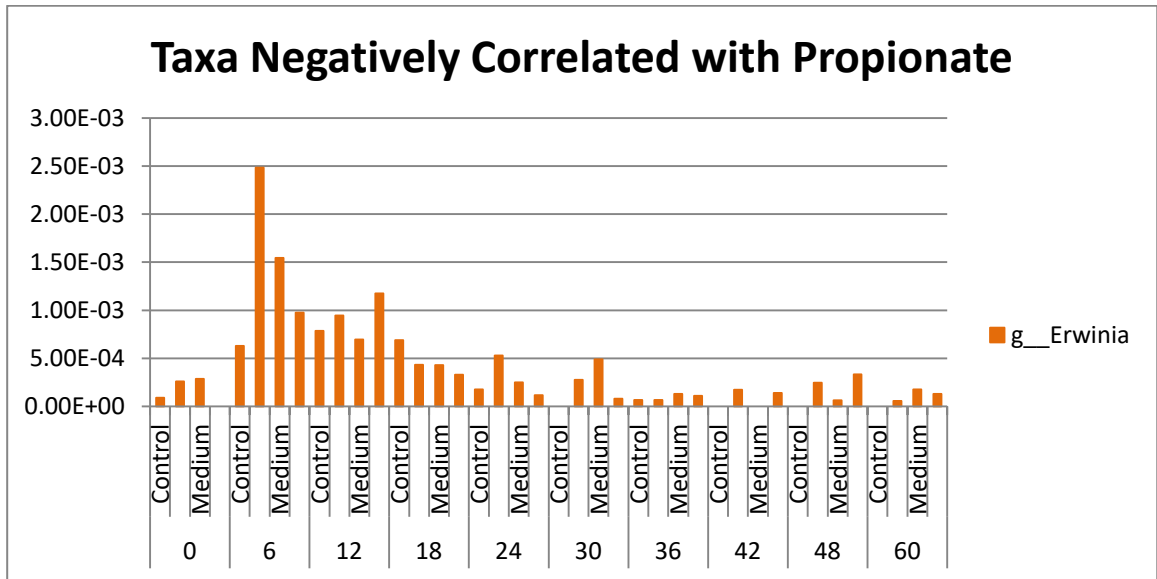


Figure 25: Taxa negatively correlated with propionate over the time-course.

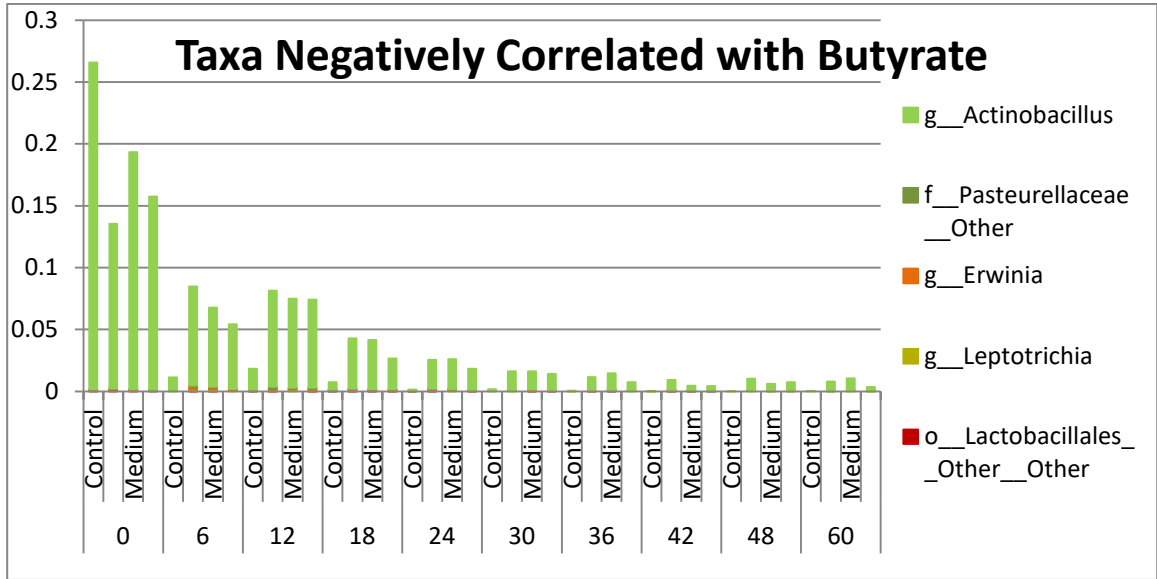


Figure 26: Taxa negatively correlated with butyrate over the time-course.

3.4.3 Drug Affected Taxa Correlation Data

The following figures summarize and illustrate taxa that did not follow a strict positive or negative correlation across the time-course. Figures were generated in R.

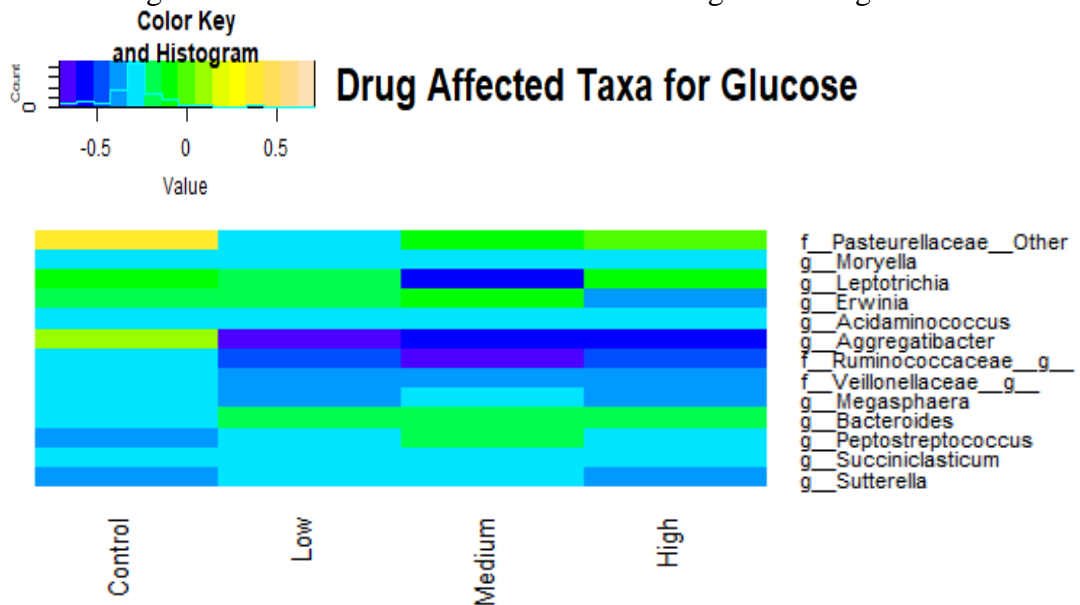


Figure 27: Drug Affected Taxa for Glucose

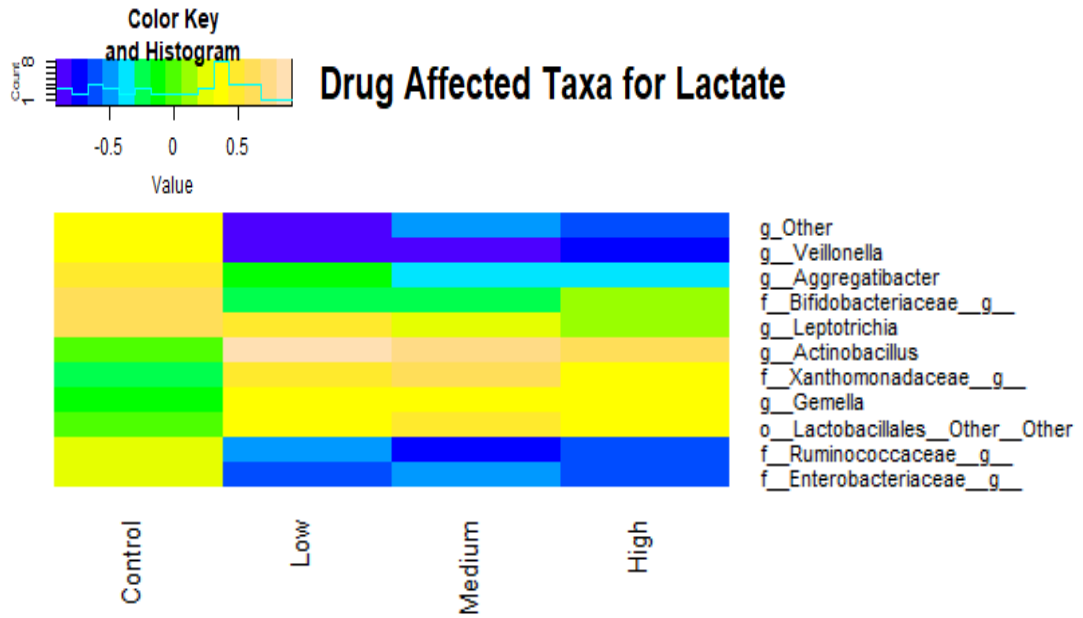


Figure 28: Drug Affected Taxa for Lactate.

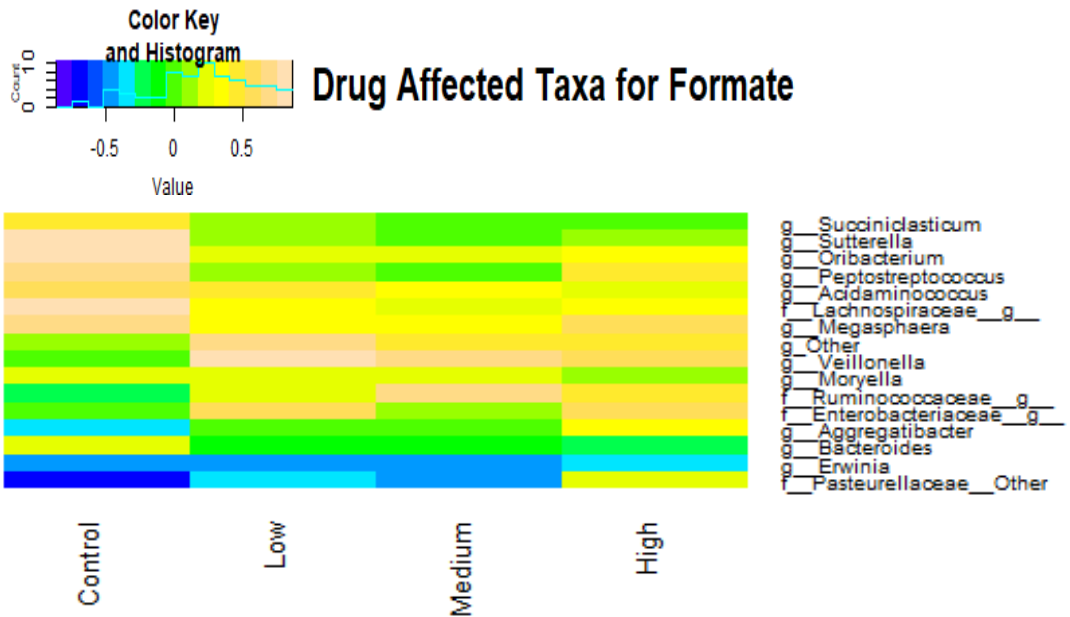


Figure 29: Drug Affected Taxa for Formate.

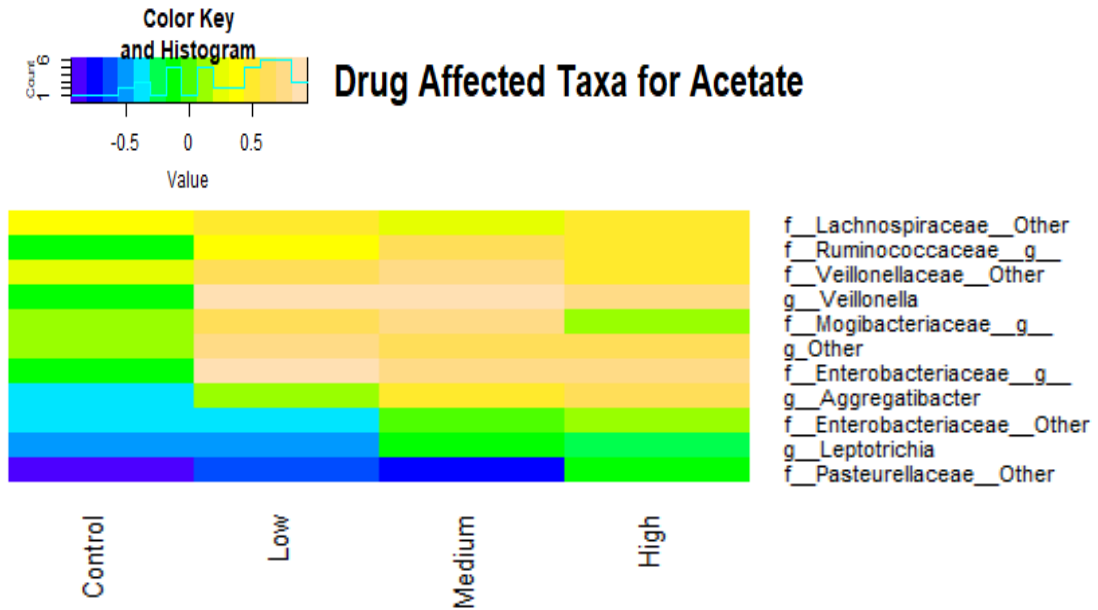


Figure 30: Drug Affected Taxa for Acetate.

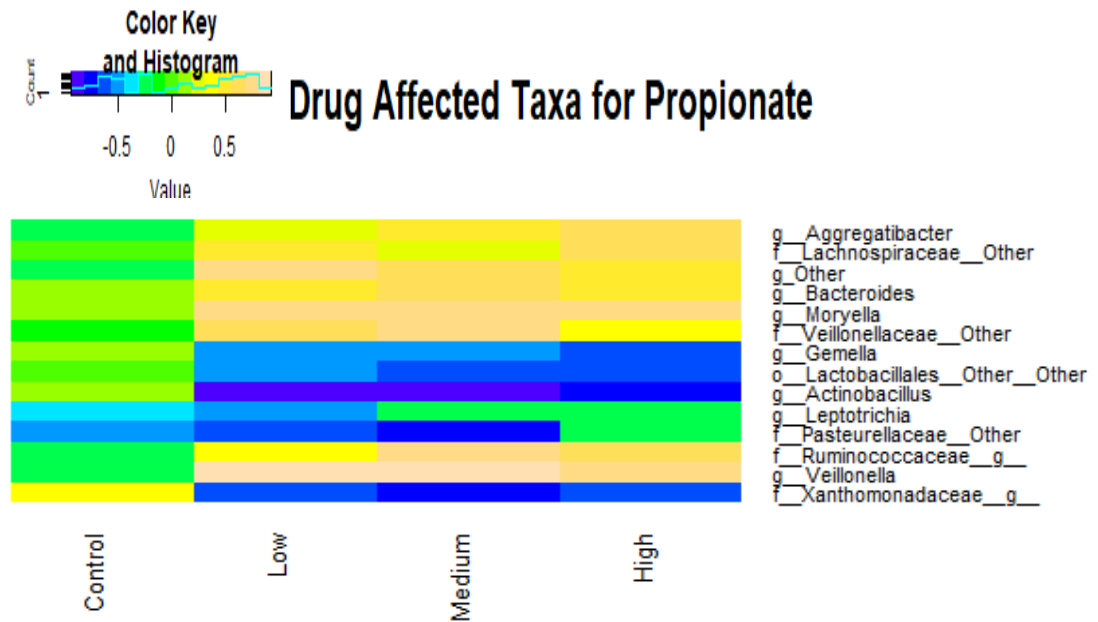


Figure 31: Drug Affected Taxa for Propionate

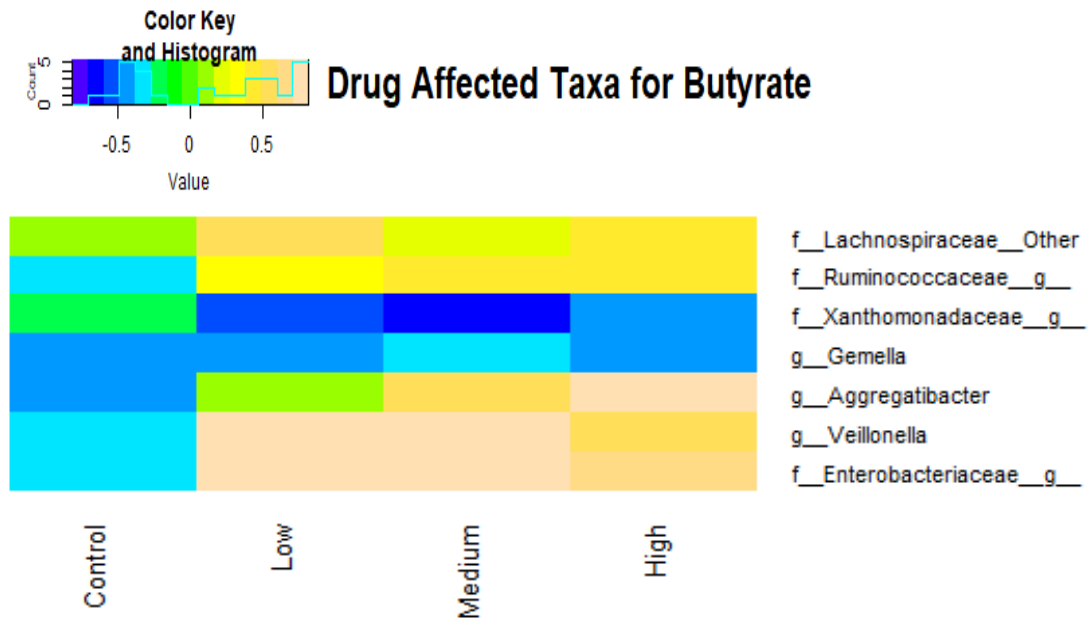


Figure 32: Drug Affected Taxa for Butyrate.

Chapter 4

Discussion

4.1 Experimental Goals

This study aimed to explore and characterize the relationships between the bacterial populations in the equine gastric microbiome and their interactions with the NSAID, firocoxib. This analysis was done utilizing data collected from a 48-hour time-course, experimental observations, HPLC, and 16S rRNA sequencing. This discussion aims to analyze the trends seen in aforementioned data and predict interactions between taxa and the administered treatment as well as characterize any observed dose effects of the treatment on the taxa.

4.2 Taxa Analysis

The most abundant taxa in the horse utilized for this study were of the phyla *Firmicutes*, *Proteobacteria*, and *Bacteroidetes*, Table 2 and Figure 13; this aligns with the previously mentioned studies of the equine gastric taxonomic population.^{9,10} Based on this alignment, the horse used for this study has a gastric microbiome that is representative of a normal horse.

Taxonomic abundance data output from QIIME was used for statistical analyses for this study. The two most important statistical tests were DESeq and JAMOVI ANOVA. The DESeq statistical test, Table 5, allowed the determination of significant differentially abundant taxa due to treatment with firocoxib. This test demonstrated which taxa that were significantly affected in their abundance because of

the presence of firocoxib in their environment. Based on the results of this test, no dose effects were observed, taxa abundance was affected by the presence of the drug, but taxa abundance was not significantly affected between doses. Only one taxa, *Lactobacillus__Other__Other*, was differentially abundant between the control, low, medium and high doses of firocoxib. Six taxa were differentially abundant between the control and low dose of firocoxib, thirteen taxa were differentially abundant between the control and medium dose, and nine taxa were differentially abundant between the control and high dose of firocoxib. These results demonstrate a drug effect on the abundance of the gastric microbiome.

The JAMOVI ANOVA statistical test was utilized to analyze the taxonomic data for significant differences between taxa abundance and time. Of the 43 taxa, only three taxa, *f__Bifidobacteriaceae_g_* and *f__Lachnospiraceae__Other*, and *g__Catonella* did not have significant differences in abundance over time. Ten taxa, mentioned previously, were later removed from consideration due to having less than a 0.001 relative abundance for all samples. Due to sample numbers, statistical analyses for significant differential abundance between individual time-points were unable to be completed.

4.3 Interpreting Results by Metabolites

This study consisted of three major component, observational experimental data, HPLC metabolite data, and taxonomic data. The combination of these components allowed for the observation of trends and or correlations present. The concentrations of six metabolites were tracked using HPLC and the following sections combine this data with the taxonomic data in order to attempt to establish

relationships. Figure 14 illustrates some of the most common bacterial metabolic pathways with metabolites that were tracked via HPLC.

4.3.1 Glucose

Figure 5 represents the average trend of glucose over the time-course. Low, medium, and high dose data was merged and averaged after statistical analysis determined that there were no significant differences in glucose concentrations between treatments. Both the control and dose glucose concentrations drop sharply between hours 0 and 6, an indication of the microbial metabolism of glucose. Glucose concentrations in the uninoculated vials remained between 14 and 18 mmoles which is consistent with a lack of bacterial contamination. The pH dropped slightly between time zero and 18 which initially does not seem congruent with bacterial fermentation of glucose into energy. However glucose is the precursor to several other metabolites tracked during the study, namely lactate. This fact coupled with the slight drop in pH, sharp decrease in glucose concentration, and an increase in gas production between time 0 and 6 (Figure 6) supports the conclusion that glucose was either taken up by the bacteria for rapid metabolism or it was transformed into directly into other metabolites, such as lactate.

Bacteria in Figure 15 were found to be positively correlated with glucose meaning that the relative abundances of these bacteria followed the same trend as the concentrations of glucose over the time-course. As the glucose decreases so do the abundances of the bacteria. These bacteria most likely utilize glucose as their sole source of energy for metabolism so when glucose is depleted these bacteria diminish in their abundance. The bacteria present in Figure 21 are negatively correlated with glucose meaning that their relative abundances do not follow the same trend as

glucose concentrations over time. For these bacteria their relative abundances increase as glucose concentrations decrease over time. These bacteria are likely involved in glucose utilization and transformation into other metabolic products such as lactate. The bacteria may also utilize other metabolic end products not tracked by HPLC, such as succinate, which are produced by the bacteria that are positively correlated with glucose as sources of energy.

Figure 27 illustrates the bacteria that did not follow a strict positive or negative correlation over the time-course. These bacteria were affected by the presence of firocoxib in their environment. *Erwinia* and *Leptotrichia* have no correlation to glucose concentration in the control and low dose treatment groups and opposing negative correlations in the medium and high dose treatment groups. *Erwinia* has a negative correlation to glucose in the high dose treatment and *Leptotrichia* has a strong negative correlation to glucose in the medium dose treatment. It appears that the populations of both of these bacteria increase with increasing concentrations of the drug indicating that the drug creates a favorable environment for them. *Pasturellaceae* is positively correlated with glucose in the control treatment, negatively correlated with glucose in the low dose treatments, and has no correlation with glucose in the medium and high dose treatments. When not treated with firocoxib the population of *Pasturellaceae* follows the same trend and glucose concentration though the time-course. However introducing firocoxib to the environment seems to promote the growth of these bacteria, and while there is no distinct correlation in the higher dose treatments, the cooler colors lean more towards a negative correlation than a positive one. *Rumminococcaceae*, *Veillonellaceae*, and *Megasphaera* have a weak negative correlation to glucose in the control treatment and a markedly negative correlation to

glucose in the treatment vials. Populations of these bacteria increase as glucose concentrations decrease and as drug concentrations increase. These bacteria, who are all members of the phylum *Firmicutes* are known to utilize glucose and lactate to produce butyrate, acetate, and propionate.³²⁻³⁶ This trend could be indicative of several scenarios. These bacteria may have found a way to utilize firocoxib as a novel energy source. Increasing concentrations of firocoxib may inhibit the growth of important competitors of these bacteria. The elimination of these competitors may allow these bacteria to grow in their place. Along that same vein increasing concentration of firocoxib may change in the environment in way that were not measured in this study making it more favorable to these bacteria. Conversely *Aggregatibacter* has a weak positive correlation to glucose in the control meaning that populations of these bacteria decrease along with glucose concentrations throughout the time-course. Yet they also a strong negative correlation in dosed treatments indicating that their growth helped by the presence of the drug. *Aggregatibacter* has the strongest negative correlation at the medium dose and slightly less strong correlations in the low and high doses. The exact reasons behind these dose effects are unknown but are mostly likely similar to the aforementioned group. *Bacteroides* exhibits a negative correlation to glucose in the control treatment but no correlation in the dosed treatments indicating that their growth may be prevented by the addition of the drug. But because *Bacteroides* does not exhibit a positive correlation, these results are inconclusive as to what effect firocoxib concentrations have on these bacteria. *Peptostreptococcus* also has a negative correlation to glucose in the control, a weak negative correlation to low and high dose treatments and no correlation to glucose in the medium treatment. This data suggests that these bacteria are sensitive to the concentration of firocoxib in the

environment. These bacteria may be partially inhibited by firocoxib at the medium dose. More work needs to be done to see why these bacteria seem to grow at low and high concentrations of the drug but it may be due to the inhibition of the growth of competitors allowing these bacteria to grow. *Moryella*, *Acidaminococcus*, *Succiniclasicum*, and *Sutterella*, all have no correlation or a very weak negative correlation to glucose in the presence of firocoxib. These bacteria are either not affected by the presence of the drug or benefit from the presence of the drug. The addition to firocoxib to the environment of these bacteria may inhibit the growth of their competitors allowing these bacteria the opportunity to proliferate.

While the drug effects on bacterial populations are interesting their true importance is unrealized until metabolomic data is added in. The majority (7) of the bacteria seen in Figure 25 are part of the phylum *Firmicutes*. Members of this phylum are known to utilize glucose and other metabolites to produce acetate, propionate, and butyrate.³⁷⁻³⁹ This correlated with the trends described in the previous paragraph in which members of the phylum (*Moryella*, *Acidaminococcus*, *Ruminococcaceae*, *Veillonellaceae*, *Megasphaera*, *Peptostreptococcus*, and *Succiniclasicum*) a general negative correlation with glucose concentration, which indicates that they are indeed utilizing glucose. The second most prominent phylum in Figure 25 was *Proteobacteria*. Members of this phylum including *Pasturellaceae*, *Erwinia*, *Aggregatibacter*, and *Sutterella* are known to ferment both glucose and lactate to produce lactic acid, acetic acid, propionate, succinate, and formate.⁴⁰⁻⁴² There is some variation in the correlation trends between the members of this phylum, however these variations are most likely due to difference preferences between the bacteria of which metabolite they will utilize first. There were two other phyla present in this group in

addition to *Firmicutes* and *Proteobacteria* and they were *Fusobacteria* and *Bacteroides*. Both *Leptotrichia* and *Bacteriodes* the respective members of the aforementioned phyla showcase trends closer to no correlation or extremely weak negative correlations to glucose. While these bacteria do utilize glucose they make preferentially utilize other metabolites to complete their metabolic cycles such as succinate.³²

4.3.2 Lactate

Figure 6 represents the average trend of lactate over the time-course. Low, medium, and high dose data was merged and averaged after statistical analysis determined that there were no significant differences in lactate concentrations between treatments. Average gas volume was also superimposed onto the graph as an indicator of microbial activity. The control treatment follows the trend in gas production very closely between time 0 and 6, with peak lactate concentration and gas volume being seen at time 6. After time 6 lactate and gas production drops off sharply with gas levels persisting longer than lactate concentrations. Dosed treatment vials have a higher initial concentration of lactate (7 mmole) compared to the control treatment (1 mmole). The dose average lactate concentration increases between time 0 and 6 just like the control treatment but does not peak as high with dose treatment lactate concentrations peaking at 12 mmole and control treatment lactate concentrations peaking at 16 mmole. Lactate concentrations in both the control and dose treatment are zero by time 18. In general the dosed trend in lactate concentration is less severe than the control lactate concentration. Uninoculated vials saw no change in lactate concentrations throughout the time course, a further indication of a lack of bacterial contamination. The pH as previously mentioned and shown in Figure 5 dropped

slightly between time zero and 18 indicating bacterial metabolism and production of acids like lactate. Figure 16 summarizes taxa that are positively correlated with lactate. The abundances of these taxa follow the same trend as lactate increasing exponentially at time 6 and then decreasing to basal levels by time 30. These bacteria most likely utilize lactate as their sole source of energy and once lactate concentrations are depleted they run out of a carbon source for metabolism evidenced by the increasing concentrations of both acetate and propionate. Figure 20 summarizes the taxa that are negatively correlated with lactate levels. The abundances for these taxa are almost non-existent from time 0 to time 6 and then begin to increase at time 12 and continue to increase throughout the duration of the time-course. The bacteria in the control treatment are consistently higher than the treatment groups beginning at time 18, however the abundances in the control group are lower than the treatment indicating a drug effect on the bacteria. The rise and fall of the bacterial abundances in the treated groups mirrors the more sedate increase and decrease of lactate concentration in the treated groups in Figure 6. Bacteria negatively correlated with lactate are likely lactate producers that cannot tolerate acidic conditions.

Figure 28 illustrates bacteria that did not follow a strict positive or negative correlation throughout the time-course. Taxa that were grouped in the *Other* designation, as well as *Veillonella*, *Ruminococcaceae*, and *Enterobacteriaceae* had no correlation with lactate in the control treatment but show a persistent negative correlation with the addition of firocoxib. In addition *Ruminococcaceae* appears to have a dose effect, with the negative correlation of increasing as dose increases. This negative correlation suggests that the bacteria are negatively affected by the addition of firocoxib to their environment as their populations decrease as the concentration of

lactate increases. *Actinobacillus*, *Xanthomonadaceae*, *Gemella*, and *Lactobacilales* had no correlation to lactate in the control treatment but increasingly positive correlations as the doses of the drug increased. The addition of the drug seems to have made the environment more favorable to the bacteria and encouraged them to proliferate either by providing a novel source of nutrients or by eliminating or inhibiting the growth of bacteria that are competitors to the bacteria previously mentioned. *Aggregatibacter*, *Bifidobacteriaceae*, and *Leptotrichia* all showcase a weak positive correlation in the control and an increasingly negative correlation in the treatments, although only *Aggregatibacter* had truly significant negative correlation. Nonetheless, the common trend indicates that the populations of these bacteria opposed the trend of lactate concentration across the time-course. Introducing firocoxib to their environments seems to have detrimentally affected them in some way causing their populations to decrease. Unlike with glucose there was equal representation from phyla groups *Firmicutes* and *Proteobacteria*. Members of the former phylum include *Veillonella*, *Gemella*, *Lactobacillus*, and *Ruminococcaeae*. These bacteria utilize both glucose and lactate in order to produce lactic acid, acetate, propionate, and butyrate.³²⁻³⁵ These metabolic pathways correlate with the correlations seen in Figure 25 with *Veillonella* and *Ruminococcaceae* showing a negative correlation with lactate concentrations, meaning that their populations follow the opposite trend that lactate concentration does. These two bacteria are more likely use glucose in order to make lactic acid or one of the other previously mentioned metabolic products. *Gemella* and *Lactobacillus* on the other hand show a positive correlation with lactate concentrations indicating that their populations follow the trend of lactate levels in the environment. These bacteria are most likely the lactate utilizers.^{33,34} Members of the phyla *Proteobacteria*

include *Aggregatibacter*, *Actinobacillus*, *Xanthomonadaceae*, and *Enterobacteriaceae*. These bacteria utilize glucose and other five and six carbon sugars in order to make acetate, propionate, succinate, and formate.^{36,42} *Aggregatibacter* and *Enterobacteriaceae* show a positive correlation to lactate in the control treatment but increasingly negative correlations as firocoxib dose increases. The populations of these bacteria are decreasing in relation to lactate *Actinobacillus* and *Xanthomonadaceae* on the other hand show a positive correlation to lactate in dosed vials indicating that the presence of firocoxib benefits their growth by inhibiting their competitors or by another unknown mechanism.

4.3.3 Formate

Figure 7 represents the average trend of formate over the time-course. Low, medium, and high dose data was merged and averaged after statistical analysis determined that there were no significant differences in formate concentrations between treatments. Average lactate concentration was superimposed on this graph to see if there was any relationship between the two metabolites. Formate concentrations begin to rise from the beginning of the time-course but undergo a rapid increase at time 18, which is right around when lactate concentrations begin to diminish. There are also two peaks in the control concentrations of formate, one at time 12 and another at time 39. The second peak in formate production could be due to the formate producers utilizing another energy source in order to produce the metabolite. It is important to note the variation in the scale of concentration as well. Lactate concentrations along the right vertical axis go up to 20mmole while the formate concentrations along the left axis only go up to 2mmole. While it appears that there is a relationship between the two metabolites, this is in fact due to skew from figure

organization. The relationship between the control treatment and lactate production is important in illustrating the normal function of the gastric microbiota what is more interesting is the lack of formate production in the treatment vials. In the control formate concentrations started at about 0.1mmole whereas in the treatment vials formate barely peaked at 0.1mmole. It is clear even from the metabolite data that there was a marked dose effect on the production of formate. Formate concentrations in the uninoculated vials remained undetectable, which again is consistent with a lack of bacterial contamination.

Bacteria in Figure 17 were found to be positively correlated with formate meaning that the relative abundances of these bacteria followed the same trend as the concentrations of formate over the time-course. As the formate concentrations increased so did the abundances of the bacteria. These bacteria most likely produce formate from some metabolic precursor. The bacteria present in Figure 23 were negatively correlated with formate meaning that their relative abundances do not follow the same trend as formate concentrations over time. For these bacteria their relative abundances decrease as formate concentrations increase over time. These bacteria are negatively affected by the presence of formate either due to changes in pH or due to the fact that their energy sources were depleted earlier in the time-course.

Figure 29 illustrates the bacteria that did not follow a strict positive or negative correlation over the time-course. These bacteria were affected by the presence of firocoxib in their environment. *Oribacterium*, *Acidaminococcus*, *Lachnospiraceae* and *Megaspharea* have a weak to strong positive correlation to formate concentration in the control treatment groups and decreasingly positive correlations in the treatment groups. This shift from a strong positive correlation to a weak to no correlation in the

dosed treatments seems to suggest a negative effect on bacterial populations with the addition of the drug. Although the shift from positive to no correlation is nowhere near as compelling as a shift from a positive to a negative correlation it does indicate a shift in the growth of these bacteria. *Succiniclasticum*, *Sutterella*, and *Peptostreptococcus* also have a strong positive correlation in the control group and no correlation of formate concentrations in the dosed treatments. Like the bacteria in the group previously mentioned these results are not especially compelling but do support the trend seen in Figures 15 and 21. *Other* and *Veillonella* show no correlation to formate in the control treatment but show strong positive correlations to formate in all of the dosed treatments, with *Veillonella* in particular showcasing an increasing positive correlation with increasing firocoxib concentrations. *Moryella* and *Bacteriodes* hover between weakly positive and no correlation to formate concentrations in the control and all treatments, which suggests that these two are relatively unaffected by formate. *Ruminococcaceae* and *Enterobacteriaceae* like the two previously mentioned taxa also hover around no correlation and weakly positive correlations for all treatments. However unlike the other two *Ruminococcaceae* and *Enterobacteriaceae* both show a strongly positive correlation with one of the treatment groups. *Ruminococcaceae* has a strong positive correlation to medium and high dose of firocoxib and *Enterobacteriaceae* has strong positive correlations to the low and high treatments. These trends suggest a more complex relationship between metabolism and firocoxib concentration in the environment. It could be that the drug inhibits metabolism at some concentrations but may also promote growth by negatively affecting the competitors to these bacteria. *Aggregatibacter*, *Erwinia*, and *Pasturellaceae* all exhibit a negative correlation to formate concentration in the control treatment with

Pasturellaceae having a significantly negative correlation to formate, indicating that its populations decrease as formate concentrations increase. The negative correlation becomes less strong as firocoxib concentrations increase, again suggesting that the drug has a positive effect on the populations of these bacteria. *Aggregatibacter* goes from a negative correlation to no correlation which again, although not significant does suggest a positive effect on the bacterial populations in the presence of the drug. *Erwinia* is the only group whose correlation to formate remains consistently negative regardless of treatment indicating that its populations are largely unaffected by the presence of the drug but is affected by formate in the environment.

While the drug effects on bacterial populations are interesting their true importance is unrealized until metabolomic data is added in. The majority (9) of the bacteria seen in Figure 27 are part of the phylum *Firmicutes*. Members of this phylum are known to utilize formate and other metabolites, specifically lactate, to produce acetate, propionate, and butyrate. This correlated with the trends described in the previous paragraph in which members of the phylum (*Succiniclasticum*, *Oribactirum*, *Peptostreptococcus*, *Acidaminococcus*, *Lachnospiraceae*, *Megasphaera*, *Veillonella*, *Moryella*, and *Ruminococcaceae*) have control and treatment correlations that range from strongly positive to no correlation. This is more evidence supporting a marked drug affect on the populations of these bacteria. The second most prominent phylum in Figure 27 was *Proteobacteria*. Members of this phylum (*Sutterella*, *Enterobacteriaceae*, *Aggregatibacter*, *Erwinia*, and *Pasturellaceae*) and are known to ferment both glucose and lactate to produce lactic acid, acetic acid, propionate, succinate, and formate.^{40,42} There is some variation in the correlation trends between the members of this phylum. The variation seen in this group could be due to different

metabolic pathways, but it is evident that again there is a drug effect on bacteria populations. The other phyla present in this group in addition to *Firmicutes* and *Proteobacteria* was *Bacteroides*. *Bacteriodes* utilized glucose to make butyrate and based on the trend of Figure 27 is not greatly affected by different drug concentrations but it is affected by the mere presence of the drug.

4.3.4 Acetate

Figure 8 represents the average trend of acetate over the time-course. Low, medium, and high dose data was merged and averaged after statistical analysis determined that there were no significant differences in glucose concentrations between treatments. Both the control and dosed acetate concentrations begin to increase at time 6 and experience a sharp increase between time 12 and 18. Both the control and the dose lines experience the same trend, but much like with lactate the control tends to be much sharper. It experiences a higher overall concentration and the rises and falls in concentration appear to be much more severe. The dose trend line is more moderate in comparison, rising more slowly, peaking at a lower overall concentration (1.5mmole as opposed to 2.25mmole). Acetate concentrations in the uninoculated vials remained constant, which is consistent with a lack of bacterial contamination. Lactate concentration was superimposed on the graph in an attempt to see if there was any relationship between the two metabolites. Lactate is a precursor to acetate and this is illustrated between time 6 and 18. As lactate concentration drops off acetate concentration increases. It experiences the sharpest increase between time 12 and 18, exactly when lactate experiences its sharpest decrease.

Bacteria in Figure 18 were found to be positively correlated with acetate meaning that the relative abundances of these bacteria followed the same trend as the

concentrations of acetate over the time-course. As the acetate concentrations increase so do the abundances of the bacteria. These bacteria could be utilizing acetate as an energy source. The bacteria present in Figure 24 are negatively correlated with acetate meaning that their relative abundances do not follow the same trend as acetate concentrations over time. For these bacteria their relative abundances are high when acetate concentrations are low and low when acetate concentrations are high. These bacteria are the same as those negatively correlated with formate and positively correlated with lactate, indicating that these bacteria are responsible for lactate metabolism and conversion into acetate.

Figure 30 illustrates the bacteria that did not follow a strict positive or negative correlation over the time-course. These bacteria were affected by the presence of firocoxib in their environment. *Lachnospiraceae*, *Ruminococcaceae*, *Veillonelaceae*, *Veillonella*, *Mogibacteriaceae*, *Other*, and *Enterobacteriaceae* have a weakly positive to no correlation to acetate concentration in the control treatment. All of these taxa do have a weak to strong positive correlation to acetate when firocoxib is present. The positive correlation decreases as firocoxib concentration increases, but still remains significantly positive. *Aggregatibacter* has a negative correlation to acetate in the control treatment, no correlation in the low treatment, and increasingly positive correlations in the medium and high doses. This is not only indicative of a drug effect but a dose effect as well. Without firocoxib populations of *Aggregatibacter* decrease as acetate concentrations increase, but with the addition of firocoxib *Aggregatibacter* populations increase in tandem with acetate concentration. *Leptotrichia* and *Pasturellaceae* have strong negative correlations to acetate in the control, low, and medium treatments in the case of *Pasturellaceae*. These bacteria shift from a negative

correlation to no correlation with acetate concentrations indicating that the presence of firocoxib may be beneficial to their growth.

While the drug effects on bacterial populations are interesting their true importance is unrealized until metabolomic data is added in. The majority (5) of the bacteria seen in Figure 30 are part of the phylum *Firmicutes*. Members of this phylum are known to utilize glucose and other metabolites to produce acetate, propionate, and butyrate.^{32–36} This correlated with the trends described in the previous paragraph in which members of the phylum (*Lachnospiraceae*, *Ruminococceae*, *Veillonellaceae*, and *Mogibacteriaceae*) a general positive correlation with acetate concentration. The second most prominent phylum in Figure 30 was *Proteobacteria*. Members of this phylum (*Enterobacteriaceae__Other*, *Aggregatibacter*, *Enterobacteriaceae__g*, and *Pasturellaceae*) are known to ferment both glucose and lactate to produce lactic acid, acetic acid, propionate, succinate, and formate.^{40–42} The correlation trend seen between the members of this phylum started off negative and then shifted into no correlation or a slight positive correlation. The shift from strongly negative to these other correlations indicates that these bacteria benefit from the presence of the drug. There was one other phylum present in this group in addition to *Firmicutes* and *Proteobacteria*, *Fusobacteria*. *Leptotrichia* followed the same trend as the members of the phylum *Proteobacteria*.³⁴

4.3.5 Propionate

Figure 9 represents the average trend of propionate over the time-course. Low, medium, and high dose data was merged and averaged after statistical analysis determined that there were no significant differences in propionate concentrations between treatments. Both the control and dose propionate begin to increase at time 6

with a steep slope until time 18. From there the control and dose concentrations follow the same trend, but as with lactate and acetate the control concentrations over the time course are more severe. The dose propionate concentrations have a lower peak and the slope changes are softer and more gradual, which could be an indication of the drug having a dampening effect on its production. Initial and final concentrations of propionate are divergent between the control and dose data, with the control having a higher initial and lower final concentration than the dosed data. Propionate concentrations in the uninoculated vials remain almost undetectable which is consistent with a lack of bacterial contamination. Lactate concentrations were superimposed on this graph as well to attempt to illuminate any relationship between the metabolites. Propionate, like acetate, is a product of lactate metabolism, and this is illustrated at time 6. As the control and dose concentrations of propionate begin to increase lactate has peaked and is beginning to decrease sharply. The utilization of lactate and its conversion to propionate is shown between time 6 and 18.

Bacteria in Figure 19 were found to be positively correlated with propionate meaning that the relative abundances of these bacteria followed the same trend as the concentrations of propionate over the time-course. As the propionate increases so do the abundances of the bacteria. These bacteria most likely utilize propionate as an energy for metabolism. Propionate continued to increase through the end of the experiment which is why the abundances of these bacteria did not drop. The bacterium present in Figure 25 was negatively correlated with propionate meaning that its relative abundance did not follow the same trend as propionate concentrations over time. For this bacterium its relative abundance decreased as propionate concentrations increased over time. This bacterium is likely involved in propionate production.

Figure 31 illustrates the bacteria that did not follow a strict positive or negative correlation over the time-course. These bacteria were affected by the presence of firocoxib in their environment. *Aggregatibacter*, *Lachnospiraceae*, *Other*, *Bacteroides*, *Moryella*, *Veillonellaceae*, and *Veillonella* indicate no correlation to propionate concentration in the control increasingly positive correlations with increasing firocoxib concentrations. *Gemella*, *Lactobacillus*, and *Actionobacter* have no correlation to propionate concentration in the control treatment and increasingly negative concentrations in the treatment groups. This indicated that these bacteria are negatively affected by the presence of firocoxib and their population decrease more with higher doses of firocoxib. *Leptotrichia* and *Pasturellaceae* have a negative correlation with propionate in the control, low, and medium treatment for *Pasturellaceae*. These bacteria end up having no correlation in subsequent doses of the drug, however this change from a negative correlation to no correlation may indicate a favorable change in the environment for these bacteria, allowing their populations to increase. *Xanthomonadeaceae* has a positive correlation to propionate in the control treatment but a strong negative correlation to propionate in the drug treatments. This means that the addition of firocoxib to the environment of his bacteria causes a reduction in its population.

While the drug effects on bacterial populations are interesting their true importance is unrealized until metabolomic data is added in. The majority (6) of the bacteria seen in Figure 31 are part of the phylum *Firmicutes*. Members of this phylum are known to utilize glucose and other metabolites to produce acetate, propionate, and butyrate.³²⁻³⁶ This correlates with the trends described in the previous paragraph in which members of the phylum (*Lachnospiraceae*, *Moryella*, *Veillonellaceae*, *Gemella*,

Lactobacillus, and *Veillonella*). This taxa group showcases three distinct trends. *Lachnospiraceae*, *Moryella*, and *Veillonellaceae*, are known to utilize all of the previously mentioned metabolites to produce both propionate and butyrate. *Gemella* and *Lactobacillus* are known to ferment glucose and other metabolites into lactate, which is a precursor to propionate. The second most prominent phylum in Figure 29 was *Proteobacteria*. Members of this phylum (*Aggregatibacter*, *Actinobacillus*, and *Pasturellaceae*, and *Xanthomonadaceae*) are known to ferment both glucose and lactate to produce lactic acid, acetic acid, propionate, succinate, and formate. *Aggregatibacter* shows the same trend as the first group of *Firmucuties* and the remaining *Proteobacteria* follow the same trend as the second group of *Firmicutes*. There is some variation in the correlation trends between the members of the phyla, however these variations are most likely due to difference preferences between the bacteria of which metabolite they will utilize first. There were two other phyla present in this group in addition to *Firmicutes* and *Proteobacteria* and they were *Fusobacteria* and *Bacteroides*. Both *Leptotrichia* and *Bacteriodes* the respective members of the aforementioned phyla showcase diverging trends as well with *Leptotrichia* showing a negative correlation in the control treatment and an increasing positive correlation with drug treatment. *Bacteriodes* showcases no correlation in the control treatment and an increasingly positive correlation in the dosed treatment.³⁴

4.3.6 Butyrate

Figure 10 represents the average trend of butyrate over the time-course. Low, medium, and high dose data was merged and averaged after statistical analysis determined that there were no significant differences in butyrate concentrations between treatments. Both the control and dose butyrate concentrations exhibit the

same trend from time 0 until time 18, although like with acetate and propionate, the dosed concentrations have a much more sedate change when compared to the control. After time 18 there is a massive increase in butyrate concentrations until the metabolite peaks at time 36. After it peaks it drops a little, but persists through the end of sampling. In sharp contrast the dosed concentrations of butyrate, while they do continue to increase, do so to a markedly lesser degree. This contrast between the control and treatment is indicative of a dose effect on butyrate concentrations. Butyrate concentrations in the uninoculated vials remained almost undetectable, which is consistent with a lack of bacterial contamination. Lactate was superimposed into this graph in an attempt to visualize any relationships between the metabolites. Unlike with acetate and propionate, there does not seem to be a strong relationship between butyrate and lactate.

Bacteria in Figure 20 were found to be positively correlated with butyrate meaning that the relative abundances of these bacteria followed the same trend as the concentrations of butyrate over the time-course. As the butyrate concentrations increase so do the abundances of the bacteria. These bacteria could be utilizing butyrate as a source of energy. The bacteria present in Figure 26 are negatively correlated with butyrate meaning that their relative abundances do not follow the same trend as butyrate concentrations over time. For these bacteria their relative abundances decrease as butyrate concentrations increase over time. These bacteria are likely involved in butyrate production. These bacteria may also utilize other metabolic end products not tracked by HPLC.

Figure 32 illustrates the bacteria that did not follow a strict positive or negative correlation over the time-course. These bacteria were affected by the presence of

firocoxib in their environment. *Lachnospiraceae* have no correlation to butyrate concentration in the control and a weak positive correlation to butyrate in the dosed treatments with the strongest positive correlation being in the low treatment. It appears that the presence of firocoxib may be beneficial to the growth of these bacteria or that the presence of the drug affects the competitors of this bacteria allowing it to grow better. The correlations for all treatments hover between the range of no correlation to a weak positive correlation indicating that while this bacteria is affected by the drug in some way it is not a severe effect. *Xanthomonadaceae* exhibits the exact opposite trend as *Lachnospiraceae* for the dosed treatments. *Xanthomonadaceae* has no correlation to butyrate concentration in the control treatment but an increasingly negative correlation in the dosed treatments with the most negative correlation at the medium dose. Populations of these bacteria are negatively correlated with butyrate concentrations meaning that they decrease as butyrate increases. *Ruminococcaceae*, *Aggregatibacter*, *Veillonella*, and *Enterobacteriaceae* show a negative correlation to butyrate concentrations in the control treatment and increasing positive correlations in the dosed treatments. This indicates that these bacteria grow better in the presence of firocoxib, especially *Aggregatibacter*. This trend could indicate that these bacteria may have found a way to use the drug as a novel source of energy or that the presence of the drug inhibits the growth of competitors to these bacteria, allowing them to grow better in its presence. *Gemella* retains a consistently negative correlation to butyrate in both the control and treated groups, however the correlation becomes slightly less negative at the medium dose. This indicates a surge in bacterial growth at this dose of firocoxib, but it is difficult to say so with certainty because the correlation is still negative, just less negative.

While the drug effects on bacterial populations are interesting their true importance is unrealized until metabolomic data is added in. The majority (4) of the bacteria seen in Figure 32 are part of the phylum *Firmicutes*. Members of this phylum are known to utilize glucose and other metabolites to produce acetate, propionate, and butyrate.³²⁻³⁶ The trends seen among the members of the phylum (*Lachnospiraceae*, *Ruminococcaceae*, *Gemella*, and *Veillonella*) are variable due to their different metabolic pathways and preferential utilization of one substrate for metabolism over another. The second most prominent phylum in Figure 30 was *Proteobacteria* (3). Members of this phylum including *Xanthomonadaceae*, *Aggregatibacter*, and *Enterobacteriaceae* are known to ferment both glucose and lactate to produce lactic acid, acetic acid, propionate, succinate, and formate.^{36,40-42} There was also variation in the correlation trends between the members of this phylum and again are most likely due to variations in their preferred substrate for metabolism. Although butyrate production has not been characterized in the phylum the positive correlations seen in its members may be due to inhibition of competitors due to the presence of firocoxib.

4.3.7 Sulfur-Reducing Bacteria

Throughout the sampling process of the time-course there was a distinct “rotten egg” odor whenever gas volume measurements were taken. At time 0 and at times 48 and 60 there was no odor detected because there was no gas produced. The presence of this odor, which is indicative of sulfur or a sulfur compound, is evidence of the activity of sulfur-reducing bacteria. These bacteria, marked with an asterisk in Figure 14, were all present throughout the time course, as seen in Figure 12.

In this metabolic pathway sulfate is reduced to H₂S during anaerobic respiration. Bacteria such as *Megasphaera*, *Veillonella*, and *Bacteroides* use sulfate as a terminal electron acceptor where as other bacteria use oxygen as their terminal electron acceptor. As illustrated by Figure 12 both *Bacteroides* and *Veillonella* were present throughout the time-course and *Megasphaera* appeared at time 18. The presence of the rotten egg odor throughout the entirety of the time-course is evidence that these bacteria were actively reducing sulfate in the serum vials.³²⁻³⁶

Chapter 5

Conclusion

5.1 Conclusions

The introduction of firocoxib to the equine gastric microbiome causes changes to the concentrations of the metabolites produced as well as the abundances of taxa groups over the time-course. These variations in the concentrations of the metabolites indicated changes in the bacterial metabolism which in turn may have had worse effects on the bacterial populations. Although it is difficult to conclude whether or not the addition of firocoxib to the gastric environment is truly deleterious without metabolomics data, the dampening of the production of the metabolites is an indicator of changes in metabolism. The microbiome exists due to the delicate harmony between the bacterial species that populate it and the metabolic products that they utilize and produce. Disruptions to this harmony have the potential to damage the microbiome and negatively affect the host, in this case, the horse. Although it has been postulated that preferential COX-2 inhibitors, such as firocoxib, are less damaging to the horse, it has been shown that they still cause gastric ulcers in horses.⁴³ Independent of their affect on gastric and mucosal epithelium Figures 6-10 show a dampening of metabolite production over the course of the time-course and Figures 13-24 show differences between the relative abundances of bacterial populations between the control and dosed treatments. While the same bacteria are still present it is clear that these variations in relative composition of the populations between the

control and dosed treatments have an effect on metabolite production, conversion, and utilization.

Furthermore, these changes in the relative abundances in the bacterial populations between the control and dosed treatments can have more profound physiologic effects. The bacteria present in the gastric microbiome are involved in glucose metabolism and the products of this metabolism, specifically acetate, propionate, and butyrate and affect the microbiome present in the hindgut. Butyrate, for example, is the primary energy source for colonocytes and is critical to the maintenance of a healthy hindgut in horses.³⁹

5.2 Future Directions

The conclusions presented are based off the evidence from a single 48 hour time-course with gastric fluid collected from a single, healthy horse. Although the basal bacterial populations are in line with previous work done to characterize the equine gastric microbiome this study is not representative of all horses.^{9,10} Repetitions of this time-course work needs to be done in order to see if the trends seen in this data are truly representative of the effects of firocoxib on the equine gastric microbiome. And while HPLC analysis is able to track the trends of known metabolites over the time-course, it is not able to track the drug and degradation products of its metabolism in the environment. Supernatant samples have been sent out for further metabolomics analysis. The results of this analysis will not only elucidate any changes that the bacteria cause to the drug as it interacts with them but it may also illustrate deeper metabolic relationships between the bacteria present in the microbiome. More targeted HPLC analysis is also required to distinguish butyrate from ethanol. For firocoxib in particular ethanol was another metabolite that was tracked throughout the time-course

via HPLC; however its peaks were only distinguishable from butyrate for the drug treated samples not in the control. Due to the lack of a control trend to track throughout the time-course ethanol was excluded from this analysis.

Another issue faced in this study was a lack of statistical power in order to analyze relative sequence abundance by time. More samples need to be sequenced in order to perform the ANOVA that would show if relative abundance changes between time points are statistically significant. In addition cell counts should be conducted at every sampling. In addition cell count samples should be stained with PMA in order to have a ratio of live cells to total number of cells in the sample. pH of the samples should be measured with a pH meter rather than litmus paper to reduce the propensity of human error in reading the colors and in order to characterize minute changes in the pH of the samples that litmus paper cannot detect. All samples should be stored in a -80 freezer in order to preserve sample integrity.

REFERENCES

1. Admin, Maltaweel & EricLambrecht. How has the Role of Horses Changed in Human Societies? *Daily History.org* (2018).
2. Austin, G. Shaping Civilizations: The Role of the Horse in Human Societies. *The Equine Heritage Institute*
3. Hintz, H. F. & Cymbaluk, N. F. Nutrition of the Horse. *Annu. Rev. Nutr.* **14**, 243–267 (1994).
4. USDA, A. Equine Demographics 2015.pdf. (2017).
5. Equo. The Horse Industry by the Numbers. *Equo* (2017).
6. Bargai, U. THE RADIOLOGICAL EXAMINATION OF THE DIGESTIVE SYSTEM OF THE HORSE. (University of Pretoria, 1971).
7. Daly, K., Stewart, C. S., Flint, H. J. & Shirazi-Beechey, S. P. Bacterial diversity within the equine large intestine as revealed by molecular analysis of cloned 16S rRNA genes. *FEMS Microbiol. Ecol.* **38**, 141–151 (2001).
8. Kern, D. L., Slyter, L. L., Leffel, E. C., Weaver, J. M. & Oltjen, R. R. Ponies vs. Steers: Microbial and Chemical Characteristics of Intestinal Ingesta. *J. Anim. Sci.* **38**, 559–564 (1974).
9. Perkins, G. A. *et al.* Equine Stomachs Harbor an Abundant and Diverse Mucosal Microbiota. *Appl. Environ. Microbiol.* **78**, 2522–2532 (2012).

10. Costa, M. C. *et al.* Characterization and comparison of the bacterial microbiota in different gastrointestinal tract compartments in horses. *Vet. J.* **205**, 74–80 (2015).
11. Davis, J. L. NSAIDs: USES AND ADVERSE EFFECTS IN THE HORSE. 6
12. Rao, P. & Knaus, E. E. Evolution of Nonsteroidal Anti-Inflammatory Drugs (NSAIDs): Cyclooxygenase (COX) Inhibition and Beyond. *J. Pharm. Pharm. Sci.* **11**, 81 (2008).
13. Ziegler, A., Fogle, C. & Blikslager, A. Update on the use of cyclooxygenase-2-selective nonsteroidal anti-inflammatory drugs in horses. *J. Am. Vet. Med. Assoc.* **250**, 1271–1274 (2017).
14. Kollias-Baker, C. NSAIDS IN EQUINE MEDICINE: BEST PRACTICES. in *Proceeding of the NAVC North American Veterinary Conference* (IVIS, 2005).
15. Knych, H. K. Nonsteroidal Anti-inflammatory Drug Use in Horses. *Vet. Clin. North Am. Equine Pract.* **33**, 1–15 (2017).
16. Campbell, N. B. & Blikslager, A. T. The role of cyclooxygenase inhibitors in repair of ischaemic-injured jejunal mucosa in the horse. *Equine Vet. J.* **32**, 59–64 (2010).
17. Tomlinson, J. E. & Blikslager, A. T. Effects of cyclooxygenase inhibitors flunixin and deracoxib on permeability of ischaemic-injured equine jejunum. *Equine Vet. J.* **37**, 75–80 (2010).
18. Lewis, J. H. & Stine, J. G. Nonsteroidal Antiinflammatory Drugs and Leukotriene Receptor Antagonists. in *Drug-Induced Liver Disease* 369–401 (Elsevier, 2013). doi:10.1016/B978-0-12-387817-5.00022-4

19. Keegan, K. G. & Kramer, J. Effectiveness of administration of phenylbutazone alone or concurrent administration of phenylbutazone and flunixin meglumine to alleviate lameness in horses. **69**, 7 (2008).
20. McKELLAR, Q. A., Bogan, J. A., Fellenberg, R.-L., Ludwig, B. & Cawley, G. D. Pharmacokinetic, biochemical and tolerance studies on carprofen in the horse. *Equine Vet. J.* **23**, 280–284 (1991).
21. Kvaternick, V., Pollmeier, M., Fischer, J. & Hanson, P. D. Pharmacokinetics and metabolism of orally administered firocoxib, a novel second generation coxib, in horses. *J. Vet. Pharmacol. Ther.* **30**, 208–217 (2007).
22. Knych, H. K., Stanley, S. D., Arthur, R. M. & Mitchell, M. M. Detection and pharmacokinetics of three formulations of firocoxib following multiple administrations to horses: Firocoxib detection and pharmacokinetics in horses. *Equine Vet. J.* **46**, 734–738 (2014).
23. Barton, M. H. *et al.* Efficacy of cyclo-oxygenase inhibition by two commercially available firocoxib products in horses: Efficacy of cyclo-oxygenase inhibition by two commercially available firocoxib products. *Equine Vet. J.* **46**, 72–75 (2014).
24. Landoni, M. F. & Lees, P. Comparison of the anti-inflammatory actions of flunixin and ketoprofen in horses applying PK/PD modelling. *Equine Vet. J.* **27**, 247–256 (1995).

25. Chay, S., Nugent, T., Blake, J. W. & Tobin, T. The Pharmacology of Nonsteroidal Anti-Inflammatory Drugs in the Horse Flunixin Meglumine Banamine. *Equine Pract. Pharmacol.* **4**, 16–23 (1982).
26. Orsini, J. A., Ryan, W. G., Carithers, D. S. & Boston, R. C. Evaluation of oral administration of firocoxib for the management of musculoskeletal pain and lameness associated with osteoarthritis in horses. *Am. J. Vet. Res.* **73**, 664–671 (2012).
27. Cox, S. & Yarbrough, J. Determination of firocoxib in equine plasma using high performance liquid chromatography. *J. Chromatogr. B* **879**, 205–208 (2011).
28. Wright, B. Equine Digestive Tract Structure and Function. *Ministry of Agriculture, Food, and Rural Affairs* (1999). Available at: http://www.omafra.gov.on.ca/english/livestock/horses/facts/info_digest.htm. (Accessed: 23rd April 2019)
29. 40115_EQUIOXX_PIX_Update_FINAL.pdf.
30. Anders, S. & Huber, W. Differential expression analysis for sequence count data. *Genome Biol.* **11**, R106 (2010).
31. jmv | Analysis Of Variance (88 views). *Scribd* Available at: <https://www.scribd.com/document/357356441/jmv>. (Accessed: 14th May 2019)
32. Hwang, N. *et al.* Genes and Gut Bacteria Involved in Luminal Butyrate Reduction Caused by Diet and Loperamide. *Genes* **8**, (2017).
33. Kuratsu, M., Hamano, Y. & Dairi, T. Analysis of the Lactobacillus Metabolic Pathway. *Appl Env. Microbiol* **76**, 7299–7301 (2010).

34. Gemella morbillorum - microbewiki. Available at:
https://microbewiki.kenyon.edu/index.php/Gemella_morbillorum. (Accessed: 9th May 2019)
35. Shaping the Metabolism of Intestinal Bacteroides Population through Diet to Improve Human Health. Available at:
<https://www.ncbi.nlm.nih.gov/pmc/articles/PMC5339271/>. (Accessed: 9th May 2019)
36. Xanthomonas campestris - microbewiki. Available at:
https://microbewiki.kenyon.edu/index.php/Xanthomonas_campestris. (Accessed: 9th May 2019)
37. Hertz, L. & Chen, Y. Integration between Glycolysis and Glutamate-Glutamine Cycle Flux May Explain Preferential Glycolytic Increase during Brain Activation, Requiring Glutamate. *Front. Integr. Neurosci.* **11**, (2017).
38. Chang, Y.-J. *et al.* Complete genome sequence of Acidaminococcus fermentans type strain (VR4T). *Stand. Genomic Sci.* **3**, 1–14 (2010).
39. Rivière, A., Selak, M., Lantin, D., Leroy, F. & De Vuyst, L. Bifidobacteria and Butyrate-Producing Colon Bacteria: Importance and Strategies for Their Stimulation in the Human Gut. *Front. Microbiol.* **7**, (2016).
40. Pasteurellaceae - an overview | ScienceDirect Topics. Available at:
<https://www-sciencedirect-com.udel.idm.oclc.org/topics/agricultural-and-biological-sciences/pasteurellaceae>. (Accessed: 9th May 2019)

41. Erwinia - an overview | ScienceDirect Topics. Available at: <https://www-sciencedirect-com.udel.idm.oclc.org/topics/agricultural-and-biological-sciences/erwinia>. (Accessed: 9th May 2019)
42. Brown, S. A. & Whiteley, M. A Novel Exclusion Mechanism for Carbon Resource Partitioning in *Aggregatibacter actinomycetemcomitans*. *J. Bacteriol.* **189**, 6407–6414 (2007).
43. Richardson, L. M., Whitfield-Cargile, C. M., Cohen, N. D., Chamoun-Emanuelli, A. M. & Dockery, H. J. Effect of selective versus nonselective cyclooxygenase inhibitors on gastric ulceration scores and intestinal inflammation in horses. *Vet. Surg.* **47**, 784–791 (2018).

Appendix A

MEDIA AND STANDARD PREPARATION

Basal medium per liter

- 4 g of glucose ✓
- 292 mg of K_2HPO_4 ✓
- 292 mg KH_2PO_4 ✓
- 480 mg of $(NH_4)_2SO_4$ ✓
- 480 mg of NaCl ✓
- 100 mg of MgSO₄ ✓
- 464 mg of $CaCl_2 \cdot 2H_2O$ ✓
- 0.5 g of cysteine ✓
- 1 g of trypticase /casetone ✓
- 4 g of Na_2CO_3 ✓
- 0.5 g of yeast extract ✓
- 177 μ L of acetic acid
- 63 μ L of propionic acid
- 31 μ L of butyric acid
- 11 μ L of valeric acid -undiluted
- 11 μ L of isovaleric acid -undiluted
- 11 μ L of isobutyric acid -undiluted

we 121 μ L of HCl for media

200 μ L of Resazurin (indicator)

Add some dilute HCl to make more acidic (autoclave)

1.75 mL + 1.75 mL = 3.5 mL
 4.75 mL
 3.9 mL in HCl or the 100% acid

Stock Media

VFA's

The recipe gives you the desired concentration in the media, so you will need to calculate to determine how to mix with water make your stock. Maybe plan on adding up to 5 ml of your stock to the media, so for 500 ml of media, using $MV = MV$.

$(5 \text{ ml})(x \text{ concentration of stock}) = (500 \text{ ml final volume})(y \text{ concentration in media})$

- Butyric acid = $(5 \text{ ml})(x \text{ concentration of stock}) = (1000 \text{ ml final volume})(31 \text{ } \mu\text{L concentration in media}) = 2.067 \text{ } \mu\text{L concentration of stock}$
- Acetic acid = $(5 \text{ ml})(x \text{ concentration of stock}) = (1000 \text{ ml final volume})(177 \text{ } \mu\text{L concentration in media}) = 11.802 \text{ } \mu\text{L concentration of stock}$
- Propionic acid = $(5 \text{ ml})(x \text{ concentration of stock}) = (1000 \text{ ml final volume})(63 \text{ } \mu\text{L concentration in media}) = 4.134 \text{ } \mu\text{L concentration of stock}$
- Valeric acid = $(5 \text{ ml})(x \text{ concentration of stock}) = (1000 \text{ ml final volume})(11 \text{ } \mu\text{L concentration in media}) = 0.5502 \text{ } \mu\text{L concentration of stock}$

Actual Media Use

1. Mix media in 1000 mL erlenmeyer flask while heating and mixing on hot plate with CO₂ flowing in hungate.
2. Flush 175 mL bottles with CO₂.
3. Use electronic pipetter to pipette 75 mL into the glass 175 mL bottles with the blue tops while pumping CO₂ in them too.
4. Put in press
5. Autoclave in Liq 20 (no liquid required on bottom of tray)
6. Put into chamber to inoculate. bute

for stock media used 1.000g

Hot to just clear bottle
 to put
 put in semi-bottles
 to clear

Press
 Autoclave Liq 20

2 μ L of 100% of acetic

0.1L * 0.5 mol/L * 46.07 g/mol = 2.3035 g EtOH
 2.3035g / 789 g/ml = 1.45975 ml 100% EtOH
 Adjust volume to 50 ml

Make 500 mM propanol
 0.05L * 0.5 mol/L * 60.1 g/mol = 1.5025 g propanol
 1.5025 g / 0.785 g/ml = 1.914 ml propanol
 Adjust volume to 50 ml

Make 200 mM pyruvate
 (.025 L)(0.2 mol/L)(110.04 g/mol) = 0.5502 g

Adjust volume to 25 ml with q H₂O

Propionic Acid = (20ml) (100%)
 Do in hood
 = 148.9 mL
 or
 148.9 mL in 20 mL of solution

Acetic Acid
 174 M (x)
 174 M (x) = 20 mL (100%)
 = 2000 / 174 M
 = 11.494 mL
 100 mL stock = 114.94 mL in 20 mL

Sample #	Metabolite	[stock solution] (mM)	[final] mM	ul stock soln ↓	Vtot (ul)
1	glucose	100	20	360	1800
1	acetate	100	20	360	1800
1	formate	100	20	360	1800
1	lactate	100	20	360	1800
1	butyrate	100	20	360	1800
				ul qH2O	0

Sample #	Metabolite	[sample1] (mM)	[final] mM	ul sample 1	Vtot (ul)
2	glucose	20	10	500	1000
2	acetate	20	10	500	1000
2	formate	20	10	500	1000
2	lactate	20	10	500	1000
2	butyrate	20	10	500	1000
				ul qH2O	500

Sample #	Metabolite	[sample1] (mM)	[final] mM	ul sample 1	Vtot (ul)
3	glucose	20	2.5	125	1000
3	acetate	20	2.5	125	1000
3	formate	20	2.5	125	1000
3	lactate	20	2.5	125	1000
3	butyrate	20	2.5	125	1000
				ul qH2O	875

Sample #	Metabolite	[sample1] (mM)	[final] mM	ul sample 1	Vtot (ul)
4	glucose	20	0.25	12.5	1000
4	acetate	20	0.25	12.5	1000
4	formate	20	0.25	12.5	1000
4	lactate	20	0.25	12.5	1000
4	butyrate	20	0.25	12.5	1000
				ul qH2O	987.5

Sample #	Metabolite	[stock] (mM)	[final] mM	ul stock	Vtot (ul)
5	propanol	500	40	144	1800
5	ethanol	500	60	216	1800
5	propionate	100	40	720	1800
5	cellobiose	100	20	360	1800
5	pyruvate	200	20	180	1800
				ul qH2O	186

Sample #	Metabolite	[sample5] (mM)	[final] mM	ul sample 1	Vtot (ul)
6	propanol	40	20	500	1000
6	ethanol	60	30	500	1000
6	propionate	40	20	500	1000
6	cellobiose	20	10	500	1000
6	pyruvate	20	10	500	1000
				ul qH2O	500

Sample #	Metabolite	[sample5] (mM)	[final] mM	ul sample 1	Vtot (ul)
7	propanol	40	5	125	1000
7	ethanol	60	7.5	125	1000
7	propionate	40	5	125	1000
7	cellobiose	20	2.5	125	1000
7	pyruvate	20	2.5	125	1000
				ul qH2O	875

Sample #	Metabolite	[sample5] (mM)	[final] mM	ul sample 1	Vtot (ul)
8	propanol	40	0.5	12.5	1000
8	ethanol	60	0.75	12.5	1000
8	propionate	40	0.5	12.5	1000
8	cellobiose	20	0.25	12.5	1000
8	pyruvate	20	0.25	12.5	1000
				ul qH2O	987.5

Make 500 mM ethanol
density = 0.789 g/ml, 46.07 = molecular weight
1.454 ml EtOH (100%) ⇒ 50 ml total solution

butyrate ✓

Appendix B

HPLC PROTOCOL

Last Revised 1/06/14

University of Delaware HPLC Protocol

Reagents, Solutions and Standards:

1. HPLC Mobile Phase: In a 6L container, add 4L of DI H₂O, add 1.66mL of concentrated sulfuric acid, add 0.3 grams of EDTA. Stir and heat (80°C) in hood for 30 minutes using magnetic stirring hot plate. After that, only stir for 30 minutes at room temperature.
2. 10X Standard: In a 100mL volumetric flask, quantitatively add: 0.6g Succinic Acid, 2.0g Lactic Acid, 1g Acetic Acid, 0.5g Propionic Acid, 1g Ethanol, 1g Butyric Acid, 1g 1,2 Propanediol. Bring to volume with DI H₂O.
3. 1X Standard: Dilute 10mL of 10X standard to 100mL with DI H₂O.

Procedure:

1. Running HPLC
 - a. Purge the line between runs.
 - b. Turn on computer.
 - c. Ensure that line A is with the mobile phase. Make sure you have enough mobile phase for your run and at least 100mL extra and make sure the line rests at the bottom of the bottle.
 - d. Turn on LC20-AT, SR20-ACT, CTO 20A, RID10A.
 - e. Turn the valve on the LC20AT to rotation to the left and then push the purge button. Write in HPLC Log.
 - f. Double Click on EZStart 7.4SP3 and once it is up the machine should beep. Click OK when the wizard pops up.
 - g. Wait until the pump is done purging (won't say purging anymore) then click "pump on/off"
 - h. Click "open on/off"
 - i. Load the start up menu by following File→Method→Open→C:\EZStart\Projects\default\method\Startup.met→click open.
 - j. Click control→Single Run.
 - k. A window will pop up. Change the vial to -1. Sample ID=Start up, the method and data path fill by default.
 - l. Click "Start"
 - m. Wait 5 seconds (at least) and you will see the display say "0.2ml per minute". Close the purge valve so it is pointing vertically up and down.
 - n. Let the system run with this method for 30 minutes.
 - o. In the meantime, tell the computer which samples are where.
 - i. Minimize program
 - ii. Create new folder to store your sample data
 - iii. Open EZStart Offline
 - iv. If anything pops up, just click OK
 - v. Click File→Sequence→Sequence Wizard

Last Revised 1/06/14

- vi. Select the method from before: C:\EZStart\Projects\Default\Method\Default\Slage VFA Methods 41CB
- vii. Keep the rest as "1"
- viii. "For Acquisition" should be chosen
- ix. Hit next
- x. Don't put a sample ID
- xi. For data path, put the folder you just created to hold your data
- xii. For data file, put "Sample ID"
- xiii. For number unknowns: you run 2-3 standards times with a blank after each standard then add that to the total number of samples you have (ex: 50 sample + 3 standards → blank= 58)
- xiv. For "steps per run" do 1 unless you want to run your samples twice
- xv. Hit next
- xvi. First vial: 1
- xvii. Incremented by: 1
- xviii. Leave calibration vial empty
- xix. Autosampling injection value is 50ul
- xx. Hit next
- xxi. Make sure "clear all calibration at start of sequence" is checked
- xxii. Hit next then hit finish
- xxiii. Now you need to manually change settings for Sample ID. Add in the sample number, standard number or blank number into the Sample ID column in the same fashion it will be organized on the tray.
- p. Save this file by going to File→Method→Save as→Save it in the same folder you created earlier and the close the program.
- q. Put the autosampler tray into the machine making sure the lid is snapped. Close the door.
- r. Check to make sure that the CTO 20A temperature is 35°C and that pump is 0.6mL.
- s. File→Sequence→Open→select the file you created.
- t. Start the run.
 - i. Click "sequence run" icon
 - ii. "Sequence name" go to the folder created for study and open the sequence file you created
 - iii. Click "start"
- u. Once the machine is done and it says "run complete" (or just not "running" anymore).
 - i. Turn off the pump by pressing "pumps on/off"
 - ii. Turn off oven by pressing "oven on/off"
 - iii. Close the software
 - iv. Turn everything off: LC-20AT, SR-20A, CTO-20A, RID-10A
- v. Open the EZStart icon on the desktop.
- w. Click "peaks and groups", on the left and it will bring up the peaks and how many minutes.

Last Revised 1/06/14


- x. Close everything but the peaks/groups window and the chromatograph.
- y. Click Window→Tile horizontally.
- z. Make your peaks integrated.
- aa. Click the icon on the bottom that says "define peaks" and it will tell you to click the beginning and the end of peaks. Do so. Make sure "replace existing peaks in the table" is checked.
- bb. Click on "peaks/groups table"
- cc. Click on the names of the peaks and name them, based off of previously run standards.
 - i. Retention time: the length of the peak
 - ii. The window is a percentage of the retention time, and it increases as the time in the column goes on.
 - iii. ISTD ID=the ID of the peak to be used as an internal standard for this component
 - iv. So change the internal standard in each column to this sample's ID
 - v. Retention time update: leave it alone
 - vi. You want to quantitate area: because as time goes on the amount injected stays the same but the retention will get longer, and the curve will elongate and get smaller. This the height will change but the area stays the same
 - vii. Calibration flag will always be replace
- dd. Now that you have defined the peaks, you need to apply this to the data and the samples.
 - oo. File→Method→Save.
 - ff. To get the names on the chart: right click on the chart and select "annotations".
 - gg. You then need to tell it what your concentrations are. This will help it to tell you.
2. Downloading Your Data
 - a. Open EZStart Offline.
 - b. Locate data file by File→Data→Open→select folder you previously made to hold your data.
 - c. Click on file and open then click "Custom Report" which is located to the left of the screen.
 - d. Once in custom report, highlight the table (minus totals) and copy and paste it into an excel document.
 - e. Once copied in excel, rename it to the sample #, standard #, or blank # it is.
 - f. Save in folder where data was originally saved and then put on lab hard drive and dropbox to further analyze it on a DM basis.
 - g. Make sure to copy and paste your standard table data into the standard running tab excel sheet to that drifting of peaks can be monitored.
3. Cleaning the Column
 - a. Remove the pre column from the main analytical column
 - b. Then remove main column from the RID line
 - c. Attach main column into the reverse flow SIL line
 - d. Change mobile phase to 5% acetonitrile

Last Revised 1/06/14

- e. Set flow rate to 0.6 and run for 8 hours
- f. After 8 hours set it back to original flow/configuration and change to mobile phase again and let run for 8 hours
- g. Clean every 3,000 injections

Appendix C

DNA EXTRACTION PROTOCOL

<p>Quick-Start Protocol August 2016</p> <p>QIAamp® PowerFecal® DNA Kit</p> <p>The QIAamp PowerFecal DNA Kit can be stored at room temperature (15–25°C) until the expiry date printed on the box label.</p> <p>Further information</p> <ul style="list-style-type: none">• Safety Data Sheets: www.qiagen.com/safety• Technical assistance: support.qiagen.com <p>Notes before starting</p> <ul style="list-style-type: none">• Perform all centrifugation steps at room temperature (15–25°C)• If Solution C1 has precipitated, heat at 60°C until precipitate dissolves.• Shake to mix Solution C4 before use <ol style="list-style-type: none">1. Add 0.25 g of stool or biosolid to the Dry Bead Tube provided. Note: For fecal samples that are especially high in lipids, polysaccharides and protein (e.g. manure or some bird feces), smaller amounts of starting material (~0.10 g) may improve DNA yield and purity.2. Add 750 µl of PowerBead Solution to the Dry Bead Tube.3. Add 60 µl of Solution C1 and invert several times or vortex briefly.4. Heat the tubes at 65°C for 10 min.5. Secure tubes horizontally using a Vortex Adapter tube holder (cat. no. 13000-V1-24). Vortex at maximum speed for 10 min.6. Centrifuge the tubes at 13,000 x g for 1 min.7. Transfer the supernatant to a clean 2 ml collection tube (provided). Expect between 400 to 500 µl of supernatant.8. Add 250 µl of Solution C2 and vortex briefly to mix. Incubate at 2–8°C for 5 min. <p style="text-align: right;"></p> <p>Sample to Insight</p>	<p>Note: You can skip the 5 min incubation. However, if you have already validated the PowerFecal extractions with the incubation we recommend you retain the step.</p> <ol style="list-style-type: none">9. Centrifuge the tubes at 13,000 x g for 1 min.10. Avoiding the pellet, transfer up to 600 µl of supernatant to a clean 2 ml collection tube.11. Add 200 µl of Solution C3 and vortex briefly. Incubate at 2–8°C for 5 min. Note: You can skip the 5 min incubation. However, if you have already validated the PowerFecal extractions with the incubation we recommend you retain the step.12. Centrifuge the tubes at 13,000 x g for 1 min.13. Avoiding the pellet, transfer the supernatant to a clean 2 ml collection tube (provided). Do not transfer more than 750 µl at this step.14. Add 1200 µl of Solution C4 to the supernatant and vortex for 5 s.15. Load 650 µl of supernatant onto a MB Spin Column and centrifuge at 13,000 x g for 1 min. Discard the flow through and repeat until all the supernatant has been processed. Note: Each sample processed will require a total of three loads.16. Add 500 µl of Solution C5 and centrifuge for 1 min at 13,000 x g.17. Discard the flow through and centrifuge again for 1 min at 13,000 x g.18. Carefully place the MB Spin Column in a clean 2 ml Collection Tube (provided). Note: Avoid splashing any of Solution C5 onto the MB Spin Column.19. Add 100 µl of Solution C6 to the center of the white filter membrane. Alternatively, you may use sterile, DNA-free, PCR-grade water or TE buffer (cat. no. 17000-10). Note: Eluting with 100 µl of Solution C6 will maximize DNA yield. For more concentrated DNA, a minimum of 50 µl of Solution C6 can be used.20. Centrifuge at 13,000 x g for 1 min and discard the Spin Filter basket. The DNA in the tube is now ready for any downstream application. Note: We recommend storing DNA frozen (–20° to –80°C) as Solution C6 does not contain EDTA. To concentrate DNA see the Hints & Troubleshooting Guide. <p><small>For up-to-date training, information and product-specific instructions, see the respective QIAGEN kit handbook or user manual. Trademarks: QIAamp®, Sample to Insight®, QIAamp®, PowerFecal®, QIAGEN Group, 1704451 08/2016-18/2019/01 © 2016 QIAGEN, all rights reserved.</small></p>
---	--

Appendix D

QIIME SAMPLE SUMMARY

Num samples: 40
Num observations: 10691
Total count: 538457
Table density (fraction of non-zero values): 0.100

Counts/sample summary:

Min: 8510.0
Max: 25655.0
Median: 12859.500
Mean: 13461.425
Std. dev.: 3352.914
Sample Metadata Categories: None provided
Observation Metadata Categories: taxonomy